2024-05-01

Water Sufficiency For Organismal Function In Dryland Critical Zones

Lindsey Dacey
University of Texas at El Paso

WATER SUFFICIENCY FOR ORGANISMAL FUNCTION IN DRYLAND CRITICAL ZONES

LINDSEY R. DACEY

Master's Program in Environmental Science

APPROVED:

Anthony Darrouzet-Nardi, Ph.D., Chair

Mark Engle, Ph.D.

Hernan Moreno Ramirez, Ph.D.

Stephen L. Crites, Jr., Ph.D.
Dean of the Graduate School

WATER SUFFICIENCY FOR ORGANISMAL FUNCTION IN DRYLAND CRITICAL ZONES

by

LINDSEY R. DACEY, B.S.

THESIS

Presented to the Faculty of the Graduate School of

The University of Texas at El Paso

in Partial Fulfillment

of the Requirements

for the Degree of

MASTER OF SCIENCE

Department of Earth, Environmental, and Resource Sciences

THE UNIVERSITY OF TEXAS AT EL PASO

May 2024

ACKNOWLEDGEMENTS

First, I would like to recognize Dr. Anthony Darrouzet-Nardi's exceptional contributions to this research project. His mentorship has been invaluable throughout this research, and I am deeply grateful. I would also like to extend my thanks to Briana Salcido, Cat Court, Kalpana Kukreja, Jake Linder, Jane Martinez-Kwong, Talveer Singh, and Viridiana Orona for their support and contributions, which encouraged and helped me in the completion of this project. Finally, I am immensely grateful to my mother, Mary Dacey-Talbott, for her unwavering support and patience throughout this program and to my sister, Jordan Talbott, for her constant encouragement to pursue challenges. Thank you to the Ivey family and the Jornada Experimental Range Long-Term Ecological Research (LTER) sites for allowing access to their space and resources for data collection and analysis for this research. Backed and supported by the National Science Foundation under award #1853680 and award #2012475.

ABSTRACT

Water availability is crucial for organismal survival and growth in dryland environments, affecting both ecological interactions and carbon dynamics. The goal of this thesis is to develop soil water release curves (SWRCs) that link soil water potentials (Ψ) to soil water content (θ). Using the SWRCs, temporal soil water sufficiency curves are developed, which quantify the amount of time that dryland critical zones have enough water to sustain the physiology of organisms. These curves allow for effectively indicating water availability across different species, coverage types, and soil conditions, enhancing our understanding of water dynamics in drylands and contributing important parameters for a variety of studies. I examine the interaction between water, soil, and plant dynamics at two sites: the Ivey pecan farm in Tornillo, Texas and the Jornada Experimental Range in Las Cruces, New Mexico. I assess physical soil properties, including depth, texture, and ground cover types such as bare ground, creosote, mesquite, and grass. At the Ivey Pecan Orchard, fine and coarse sites were sampled to analyze variations in soil texture. Data from moisture sensors for the period of 2011-2021 were cross-verified with direct soil gravimetric measurements and SWRCs at corresponding depths. A corresponding adjustment in data allowed for accurate quantifications of soil moisture and subsequently conversions of these measurements into water potentials using the Fredlund-Xing (1994) model, thus providing a detailed view of moisture trends across different soil coverages and textures. At the Jornada Experimental Range, it was found that shallow soils at depths of 5 and 10 cm experienced significant increases in water loss (retained water less well), whereas deeper soils exhibited more water retention stability. Our refined data showed that the upper 30 cm of soils under creosote and mesquite shrubs typically maintained water availability above the wilting point of creosote (-6 MPa) only slightly more than 50% of the time. Thus, we conclude that shallow (0-30 cm) soils in the shrubland has insufficient

water availability for sustained plant health year-round, which is consistent with seasonal grass dieback at the site. Shrub species, such as creosote and mesquite, likely compensate with access to deeper water sources via their rooting structures. Preliminary correlations of soil moisture data with carbon exchange measured via eddy flux tower were inconclusive, but further modeling could reveal important connections between water sufficiency and net carbon balance. The development of temporal soil water sufficiency curves and their ability to predict water availability for organisms contribute to a broader understanding of organism water availability in drylands. This tool provides a solid foundation for future studies in drylands and works to advance the understanding of soil-plant-atmosphere relations in dryland critical zones.

TABLE OF CONTENTS

LIST OF TABLES

LIST OF FIGURES

LIST OF EQUATIONS

1. INTRODUCTION

The Critical Zone (CZ) is the biophysical layer ranging from the top of tree canopies to the groundwater table. Studies of the CZ focus on understanding the processes of the ecosystem below ground (Dawson et al., 2020; Richter & Billings, 2015). Within the CZ, the biological activities of dryland organisms such as plants and microbes are primary drivers of ecosystem functions such as carbon cycling (Weverka et al., 2023). Relations between plants, microbes, and the atmosphere play a vital role in determining dryland CO_2 fluxes. A broader understanding of the soil moisture quantities needed to control physiological activity levels in dryland organisms is needed, as these directly promote productivity and influence gas exchange with the atmosphere (Chenoweth et al., 2022; Nadkarni, 2008).

Precipitation plays a crucial role in shaping the structure and function of dryland vegetation due to its influences on biogeochemical processes, which has been highlighted in prior studies (Bhattachan, 2012; Garcia-Pichel & Sala, 2022; Wei et al., 2019; Chenoweth et al., 2022; Nadkarni, 2008). Accurately quantifying and understanding the influences of precipitation events on desert ecosystems can be challenging due to factors such as limited site accessibility, temperature influences on moisture measurement probes, non-localized calibration equations for moisture probes, and soil physical properties (S.U. et al., 2014; Singh, & Shojaei Baghini; 2014). Soil physical properties include porosity, texture, compaction, and water-holding capacity. Additionally, soil water content (θ) measurements can be influenced by variations in soil physical properties, ultimately affecting the quality of the data.

The Pulse Reserve Paradigm (PRP) describes how desert ecosystems are regulated by water availability, which is dictated by periodic wetting events like rainfall or snowmelt, alternating with periods of drought. These occurrences are responsible for key biological

processes in Northern Hemisphere drylands, resulting in periods of rainfall that mostly occur from October to December and July to September (Noy-Meir, 1973; Reynolds et al., 2004). The significance of these pulses varies depending on the plant species and their water consumption (Collins, 2014; Reynolds et al., 2004). Plant and microbial functional categories (species with comparable ecosystem functioning and environmental responses) and their use of available water resources define biological relevance (Reynolds et al., 2004). Carbon and energy reserves are stored in plant tissues following wetting episodes until they are depleted or the next wetting event occurs (Pérez-Ruiz et al., 2022). The soil moisture reserves in arid landscapes are crucial for storing surplus water from rainy periods and using it during subsequent droughts. The PRP is relevant for local ecosystems but also global CO_2 levels and the dynamics of land carbon. These effects are reliant on plant and biocrust net carbon uptake, a function of plant water potential (Ψ) (Noy-Meir, 1973; Darrouzet-Nardi et al., 2015; Reed et al., 2018; Garcia-Pichel & Sala, 2022; Reynolds et al., 2004).

Although it is common to collect volumetric water content (VWC) data, it is not always clear how this translates to plant water availability due to the factors such as soil texture and structure. These factors interact with the soil water content to determine the fraction of water available to organisms and more generally, the movement of water through the CZ. This availability can be quantified as soil water potential (Ψ). Water in the CZ moves via the Soil-Plant-Atmosphere Continuum (SPAC). The SPAC is a continuous pathway of decreasing water potential that promotes water movement through components such as soil, plants, and the atmosphere (Silva & Lambers, 2020). In this continuum, Ψ plays a crucial role. Water flows from areas of higher Ψ, such as soils, to areas of lower Ψ, such as plants, and produce gradients in Ψ, driving water into the atmosphere (Orlowski et al., 2023). The linkage between soil

properties and water availability is captured in soil water retention curves (SWRCs), which show the relationship between VWC and Ψ in specific materials. Soil physical properties determine the shape of the SWRC, which aids in understanding how the physical properties affect plant water availability temporally. To predict biologically available water and understand vadose zone water dynamics (Earth's subsurface above the water table where pore spaces are filled with mixtures of free-phase air, soil gas, and water), the development of SWRCs, which are specific to different soils, can be used to convert soil VWC (θ) into Ψ. The relationships found in SWRCs inform discussion on the role of soil moisture in environments more broadly (Holden & Fierer, 2005; Phillips & Castro, 2003). Water potential, Ψ, consists of the matric potential (Ψ_m), energy from the attraction between water molecules and soil particles; solute potential (Ψ_s), a measurement of solute concentrations; and the gravimetric component (Ψ_g), the influence of gravity on potential energy (Hillel, 2004). Ψ is typically reported as negative pressure (ignoring atmospheric pressure), contributing to the ability of soils with low matric potentials (i.e., highly negative) to draw water upward against gravity. Despite the more direct relevance of Ψ in controlling water available to plants, few studies have associated conversion of Ψ data from VWC to explore needed θ for organisms to be used to predict carbon cycling in dryland environments (Gałęzewski et al., 2020). For example, a soil-borne pathogen, *Fusarium culmorum*, showed a permanent wilting point (PWP) of -0.8 MPa (Cook et al., 1972); however, different organisms exhibit different wilting points. For instance, there is a documented case of an arbuscular mycorrhizal fungus exhibiting values of -21 MPa (Allen et al., 1989; Jasper et al., 1989).

Physical properties relevant to soil moisture include soil size, pore shape and arrangement, and mineral composition (Sanchez, 2019). In this research, we focus on the

physical properties of soils, which include: (i) soil texture, the relative composition of sand, silt, and clays, which make up the mineral fraction of soil (Fernandez-Illescas et al., 2001); and (ii) soil structure, which is the arrangement of soil particles into varied sizes of aggregates. These components, which often vary with depth, influence the porosity, permeability, bulk density, compaction influencing soil structure, water retention, and movement of water within soils (Osman, 2012; Sanchez, 2019). Plant species coverage types and life stages also contribute to soil moisture influence. The response of soil moisture to rainfall through interactions with soil physical properties can be used to predict responses of the ecosystem under varying environmental conditions.

In the Chihuahuan Desert, to address whether organisms have sufficient water availability to be active, we must first understand two concepts to grasp the efficiency of plant water use. One of the main goals of establishing this better connection between soil properties, water quantities, water availability, and plant activity of individual species is to better understand C balance data from sources like eddy covariance towers. This multifaceted accumulation of instrumentation has the capacity to measure the CO_2 exchange between Earth's surface and the atmosphere (Xiao, Chen, Davis & Reichstein, 2012). Net ecosystem exchange (NEE), which represents the difference between CO_2 de uptake and release by plants and other organisms, will be referenced to understand this relationship (Dusenge, Duarte & Way, 2019; Randerson et al., 2002; Lovett Cole, & Pace, 2006). NEE data is specifically referenced as a predictor of physiological activity because of its ability to detect respiration rates of CO_2 from organisms.

In this investigation, we examine soil moisture dynamics in the CZ within the Chihuahuan Desert, a cold, dry, semi-arid region in the southwestern USA. Two focus sites show different soil textures, composition, and behavior: a shrubland site along a Piedmont bajada and

an irrigated site in an alluvial valley adjacent to the Rio Grande. The overall aim of this research is to better understand the relationship between soil θ, soil Ψ, and plant activity in the dryland environments. I will enhance our understanding by using known data on the wilting points (the minimal Ψ that supports physiological activity) of soil-based organisms. By comparing ecosystem carbon exchange from eddy flux towers with Ψ calculations from soil moisture sensors, I aim to identify key relationships between water dynamics and organismal activity to predict conditions that promote physiological activity and carbon exchange with the atmosphere. We know that while sensors are often deployed, the influence of soil properties and moisture availability at particular sites are rarely combined to examine the proportion of times that key groups of organisms have enough water to be physiologically active, resulting in what we will call here *temporal soil water sufficiency curves*.

1.1 Challenges in Accurate Soil Moisture Quantification and Sensor Limitations

Accurate quantifications of soil moisture remain difficult even with soil moisture sensing approaches. Devices used at dryland sites in CZ such as capacitance-based sensors (Decagon ECH20, Decagon EC-5TE) and time domain reflectometry sensors (Campbell Scientific CS616) estimate soil moisture based on mixed dielectric permittivity of the materials they contact and offer higher temporal resolution (Koley & Jeganathan, 2020). As reported by the developers of these devices, Campbell Scientific (2011) and Decagon Devices (2010), their user manuals state that the factory calibration accuracy is ±0.025 and ±0.03 m^3 m^{-3}, respectively. However, it was found that factory-based calibration for field θ reported low accuracy for PWP and FC for all sensors tested, which included the 5TE and CS616 devices (Varble et al., 2011). Although there are many applications for these soil moisture sensors, they are often faced with inaccuracies and uncertainty when measuring soil water (Sharma et al., 2021). The presence of inaccuracies and

uncertainties leads to gaps and incorrect data relating to soil moisture, ultimately presenting challenges in physically monitoring water fluxes under unsaturated conditions. Solutions to this issue are not easy due to difficulties in calibrating sensors for site-specific conditions and variations in subsurface positioning (Seyfried et al., 2005). To achieve a basis for good observations, corrections of sensor data are needed to establish correct moisture values in natural environments and predict the θ in the gaps.

1.2 Objectives and goals

The objective of this research is to investigate and understand dynamics of water availability in dryland plant ecosystems through examining the relationship between soil Ψ and θ under differing soil physical properties. SWRCs will be developed under multiple conditions and compared to describe key soil physical and ecological properties, such as water retention trends under texture, depth, and individual species plant coverage, which affect soil Ψ. I use these properties to predict when plants and other organisms have sufficient water quantities for growth and atmospheric carbon exchange. To achieve these objectives, the following research questions are addressed:

1. How do the shape and critical values of SWRCs vary by texture, depth, and plant cover in irrigated versus shrubland dryland CZ?
2. What are the temporal dynamics of soil moisture and soil water potentials at these sites based on combined analyses of SWRCs and soil moisture sensors?
3. Given the plant Ψ responses of organisms in these systems (i.e., creosote bush, mesquite, soil microbes, and biocrusts), when and how often do these organisms have sufficient water availability to be physiologically active over a 10-year period?

4. Do these predicted intervals of physiological activities have predictive utility for ecosystem carbon exchange as measured with eddy covariance towers?

1.3 Soil Ψ and Plant Water Availability

PWP can vary among dryland organisms, depending on the species. Exceeding PWP results in hindering physiological activity at different Ψ ranges. Previously, PWP for dominant shrubs in the Chihuahuan desert, such as creosote bush (Larrea tridentata) and honey mesquite (*Prosopis glandulosa*) have been investigated. Creosote bush was found to reach -6 MPa before organism death was reported (Flint et al., 2004). The lowest reported PWP for living mesquite trees was –3.2 MPa; however, some studies have also reported –1.5 MPa as the PWP for mesquite, similar to the generic value for most plants (Fernandez-Illescas et al., 2001; Easter, 1973). Shrub species in drylands are suspected to have lower values than the standard PWP (-1.5 MPa), but the value may even be lower than what has been reported due to adaptations to dryland environments (Liu, 2003; Metergroup, 2021). Some fungi have been reported to have even lower PWP. For example, -60 MPa was reported for an Ascomycete taxon, but others are not so tolerant; *Fusarium culmorum* exhibits a PWP of -0.8 (Cook et al., 1972; Magan & Lynch 1986; Williams & Hallsworth 2009). The response of grasses to decreasing water availability varied by growth type, ranging from -3.0 MPa to -0.80 MPa. Biocrusts have been reported to have a PWP of -1.5 MPa (Sun et al., 2021), which aligns with the generalized wilting point standard of plants. Pecan trees display PWP values of –0.90 MPa, while microbes are more generally thought to have a PWP of around -0.5 MPa (Harris, 2015). Information is not complete for exact details of the PWP of all organisms, especially in drylands. However, these results supply a good baseline for when physiological activity is to be expected throughout this study.

Table 1 Estimates of minimal Water Potential values for dryland organisms to remain active.

PLANT FUNCTIONAL TYPES	SPECIES	MINIMAL WP ESTIMATES	REFERENCE
SHRUBS	Creosote (*Larrea tridentata*)	-6 MPa	Faust et al., 2006; Flint et al., 2004
	Honey Mesquite (*Prosopis glandulosa*)	-1.5 to -3.2 MPa	Fernandez-Illescas et al., 2001; Easter, 1973
GRASSES	C4	-2.0 to -3.0 MPa	Liu et al., 2003 ; Baruch & Bilbao, 1999; Qi & Redmann, 1993
	C3	-1.5 MPa	
FUNGI	*Fusarium culmorum;* Ascomycete (xerophilic) fungi	- 0.82 to -60 MPa	Cook et al., 1972; Magan & Lynch 1986; Williams & Hallsworth 2009
PECAN TREE	*Carya illinoinensis*	- 0.90 MPa	Othman et al., 2014
MICROBES	-	-0.5 MPa	Harris, 2015
MOSSES	*Plagiomnium affine (Funck) Kop; Dicranoweisia cirrata (Hedw.) Lindb..*	-1.2 to -2.5 MPa	Rütten, D. et a; (1993).
LICHEN		-28.7 to -38 MPa	Kranner, I.,et al.,2008
CYANOBACTERIA	*Microcoleus spp.*	-1.8 to -2.8 MPa	Potts et al, 1981; Brock et al., 1975

2. METHODS

2.1 Study sites

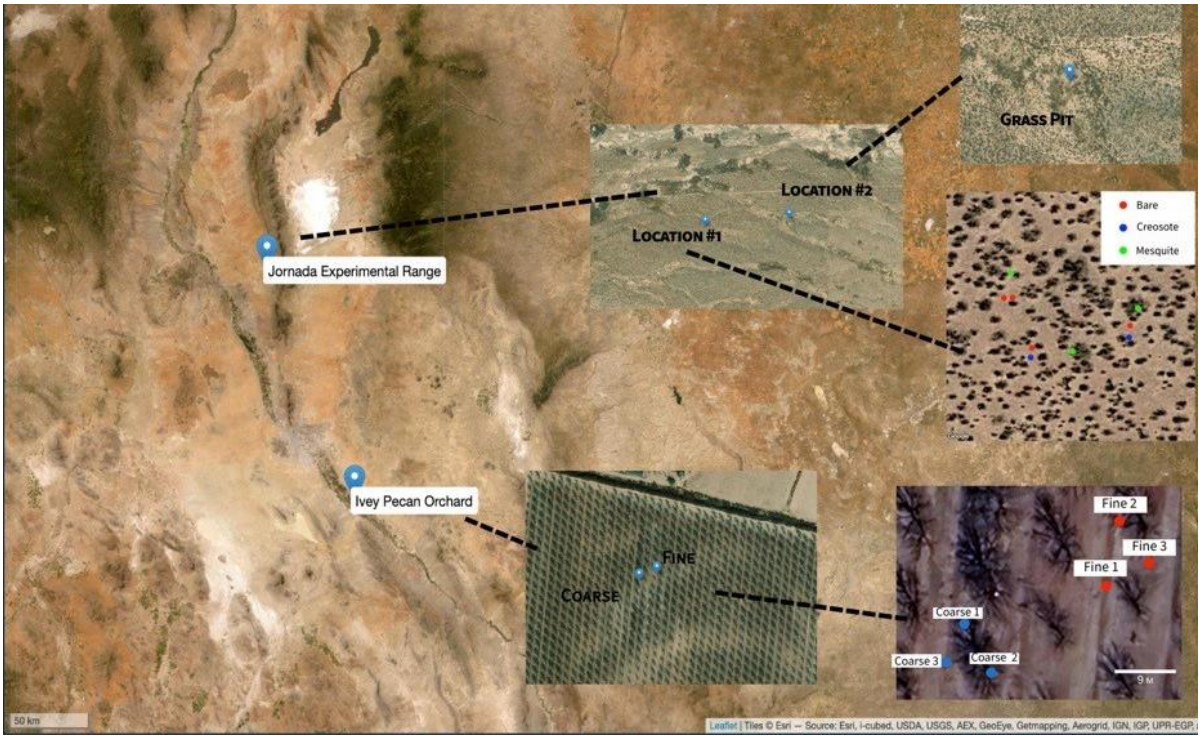

Figure 1 Map showing locations of critical zone research sites.

The study sites are in the Chihuahuan Desert, including the Jornada Experimental Range (JER), located 37 km north of Las Cruces, New Mexico (Figure 2). The typical climate of JER reflects semi-arid and arid grasslands with a mean annual precipitation of 247 mm and a large degree of sun exposure. About 65% of precipitation at the site occurs during the short and intense summer months (Mueller et al., 2007). Within the JER, our site is topographically located at the foot of the San Andres Mountains. Dominant soil types at the site are sandy loam and sandy clay loam, with dominant vegetation such as creosote bush (*Larrea tridentata*) and honey mesquite (*Prosopis glandulosa*).

2.2 Characterization of Soil Physical Properties and Water Behavior

To gain a comprehensive understanding of water behavior through the soil profile, lab methods using the following instrumentation were used to provide details on the relationship between soil physical properties and water.

An undisturbed soil core sample is used for the saturated conductivity measurements obtained from the KSAT device (METER AG, Munich), a falling head permeameter, which provides information on the rate of water movement in saturated soils, which is influenced by pore spaces of differing sizes (Meter Group, 2021). The reason for use of the KSAT was to understand the influence of soil moisture on the movement of water through fully saturated soil pores for various soil textures and structures. The incorporation of these measurements in conjunction with our SWRCs better detail the pore size distributions (porosity) and their influence of the hydraulic functions of the soils.

To develop SWRCs, two devices were used to collect soil water potential measurements across a range of soil moisture conditions. Measurements of water potential for undisturbed soil samples were determined using a Hyprop instrument (Meter Group, Pullman WA). To monitor moisture changes, this instrument uses two precision mini-tensiometers of different lengths, which are inserted into the soil. As the soil dries, these tensiometers increase in pressure due to the developing vacuum. The amount of water evaporated from the soil was able to be calculated using a hydraulic conductivity equation based on Darcy-Buckingham's law (Schindler et al., 2006):

$$K(\bar{h}) = \frac{\Delta V}{2\,A \cdot \Delta t \cdot i_m} \qquad \textit{Eq. 1}$$

Using this equation, hydraulic conductivity was calculated using: the tension average from the two tensiometers within a time interval $(\bar{h})$, the mass difference during the interval (ΔV), the surface area, (A) through which water flows, and the mean hydraulic gradient (I_m). To calculate I_m the recorded tensiometer measurements at two depths are used:

$$I_m = \frac{1}{2}\left(\frac{h_{t1,upper} - h_{t1,lower}}{\Delta z} + \frac{h_{t2,upper} - h_{t2,lower}}{\Delta z}\right) - 1 \qquad \text{Eq. 2}$$

in which the recorded tension of upper and lower tensiometer values at time (t) divided by the vertical distance between them (Δz). These calculations allow for the determination of water movement as well as the water retention capabilities of soils.

Following Hyprop measurements, three subsamples were extracted from the undisturbed soil sample for measurement using the WP4C device. This device determines the total suction of the sample based on relative humidity, which is measured in values ranging from -1 MPa to -300 MPa (María et al., 2020). By allowing the liquid and vapor phases of a sample to reach equilibrium, the vapor pressure in the chamber is measured to determine the water potential. A range of moisture conditions were attained by incrementally adding DI water to the subsamples and then processing them on the WP4C. This device required calibration using 0.5 mol/kg KCl (potassium chloride), 0.1 mol/kg KCl, and 0.01 mol/kg KCl before each use. This compound is generally stable with a well-defined relative humidity at a given temperature (Meter Group, Pullman WA). By calibrating this device, we were able to identify occurrences of contamination within the instrument or shifts in measurements.

Empirical equations such as the van Genuchten or Fredlund-Xing models can be used to predict SWRCs for a range of water potentials by fitting measured data (Van Genuchten, 1980; Fredlund & Xing, 1994). Generally, equations are continuous and are integrated into mathematical frameworks that can describe how unsaturated soils respond to the differentiating conditions (Buljak et al., 2021). Each SWRC, when modeled using an empirical equation like the Fredlund-Xing model, includes shaping parameters α (inflection point), n (slope), and, m

(curvature) are often referred to as “hydraulic parameters.” These parameters are essential for fitting the curve to measured data obtained from instruments such as the Hyprop and WP4C, which in the case of this study were analyzed using SoilView Analysis software (SoilView, 2022).

Finally, the automated soil particle size analyzer (PARIO; METER AG, Munich) device uses an integral suspension method (ISP+) to measure the particle size distribution (PSD) of soils. For PARIO ISP+ analysis, a 100 g soil sample was collected, where two subsamples of 50 g were used one subsample for the dispersion process and the other for fractionation and quantification. The analysis for particle size requires the dispersion of soils into individual particles through the introduction of a deflocculating agent (Durner & Iden, 2017). The dispersed soil is then added to an aqueous suspension in the sedimentation cylinder. Homogenization of the contents within the sedimentation cylinder is then left to settle with gravitation. Settling velocities are dependent upon the soil particle size. As particles begin to sink, segregation occurs with the sizes of the soil particles acquired (Meter Group, 2016). Additionally, wet sieving was used to conduct fractionation and quantification for each particle size. PSD is determined by measurements of the particle mass density at a specific depth and time within the sedimentation cylinder. Stokes law (Stokes, 1850) relates the time of settling to the size of particles remaining suspended in the aqueous solution. The completion time for a single PSD analysis is 2 hours and 30 minutes. These measurements can be used to plot results on a USGS soil classification triangle, which we did to aid in classification of soil samples collected from the two research sites.

To gain a more comprehensive understanding of soil water dynamics, we used these instruments to attain a better understanding of the link between soil physical characteristics from our research sites and the flow of water through the soil-plant-atmosphere continuum and, more broadly, understand water movement through the CZ. This detailed assessment of the interactions between soil texture and water availability was conducted to broaden our understanding of how various soil conditions influence water retention and movement. To address the role of soil physical properties in terms of texture, depth, and plant cover in irrigated versus shrubland dryland

sites, our sampling locations within sites incorporated varying plant covers, textures, and a range of depths from 0-30 cm (6 samples). We measured the saturated conductivity of the soil using the KSAT instrument (refer to Image C, Figure 3), and an analysis of water retention in soils was then performed using the Hyprop and WP4C instruments (refer to Figure 3, Image B). Finally, soil textures were analyzed and classified with the PARIO instrument.

Each sample was taken from specified locations within the sites consisting of differing soil physical properties such as those discussed prior. At JER, these specified locations were coverage types of four bare interspace points, two creosote coverage points, and three mesquite coverage points. At the Ivey Pecan Farm, soil texture samples were taken at three points within the fine site and three within the coarse site, corresponding with the deployed soil moisture sensors. At these locations, the samples collected from the 0 to 30 cm depth range (~100 g) were measure on the PARIO instrument. Sample collection for the KSAT and HYPROP required the use of a soil sampling ring (250 mL) for collection of undisturbed soil cores. Sampling locations were cleared of plant material or additional debris from the surfaces without disturbing the soil to preserve undisturbed conditions. The beveled edge of the sampling ring faced down into the soil, ensuring that the ring was stable and level on the soil surface. Using a sample ring insertion tool, soil compaction was able to be minimized, as the insertion tool made contact with the rim of the soil sampling ring. The insertion tool was hammered until the sampling ring was completely in the ground. Using a trowel, the surrounding soil was removed from the sampling ring without disturbing the soil within it. When the bottom of the sampling ring was able to be seen, a flat blade was placed underneath to provide stability. Once completely removed from the ground, the sampling ring was cleaned by removing excess soil from both ends. Caps were then placed on both ends of the sampling ring for transport and storage in the lab.

Gravimetric measurements of the JER soils were conducted at three depth intervals (0-10 cm, 10-20 cm, and 20-30 cm) for each core sample. It should be noted that samples intended for the development of SWRCs, saturated hydraulic conductivity measurements, and soil textural

analysis were only sampled for 0-30 cm depths (6 samples) one time for each coverage and texture type. Meanwhile, gravimetric measurements were sampled at all locations within the sites.

Collection and analysis of a spatial array of soil cores from both fine- and coarse-textured areas of the orchard were done to establish a robust framework for assessing sensor accuracy. An extensive gravimetric sampling campaign was performed for spatial moisture mapping, exclusively for the Ivey Pecan Orchard, collecting soil cores (0-100 cm) at every 10 cm depth interval from 100 points within the site. These samples were kept in airtight bags within coolers to minimize evaporation before laboratory processing, which included sieving through a 2 mm mesh and conducting a lab standard gravimetric measurement procedure and calculation to acquire ground water content (GWC). GWC includes various types of moisture content, such as hygroscopic moisture, which is the water content that soil can absorb from the air and retain against gravity (Shah and Singh, 2006), able to be converted into VWC through multiplying the bulk density value (BD). BD values were derived from the undisturbed sample cores which had known volume and weights, using the following calculation:

$$\rho_{\mathrm{bd}} = \frac{M_d}{V_d}.$$

Under oven dried conditions, ρ_{bd} is the bulk density in g cm^{-3}, M_d is the mass of the sample in grams, and V_d is the total volume of the sample in cubic centimeters (Airori et al., 2022). Soil porosity is the fraction of pore space not occupied by soils (Nimmo, 2005); these estimates were made using the following calculation (Hillel, 2004):

$$f = \frac{V_f}{V_t},$$

where porosity index estimate f is the dividend of Volume of pores (V_f) by the total volume of sample (V_t).

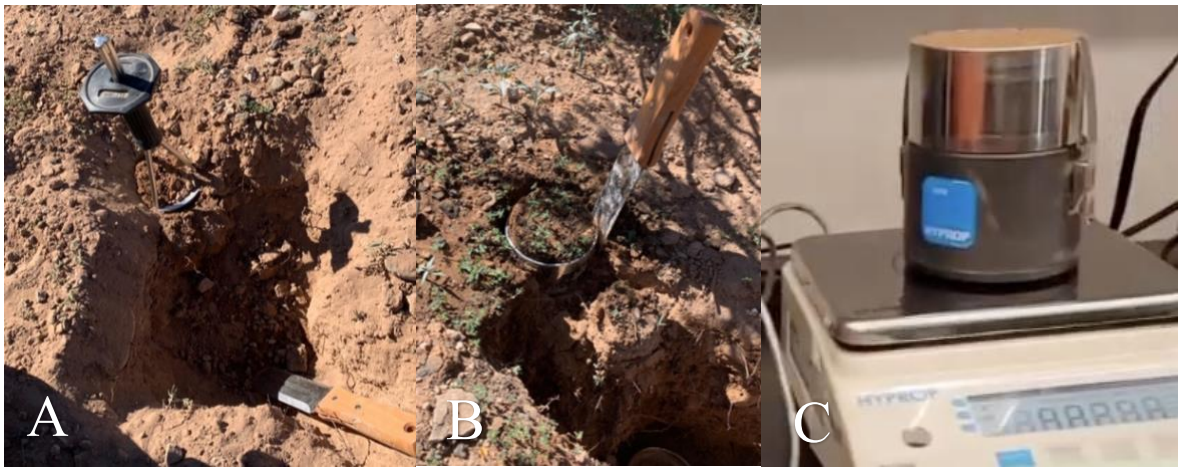

Figure 2 (A) Collecting the soil core (5-10 cm) from the bare coverage; (B) Collecting the soil core (0-5 cm) under the shrub; (C) Hyprop setup with sample

2.3 Soil Water Retention Curves

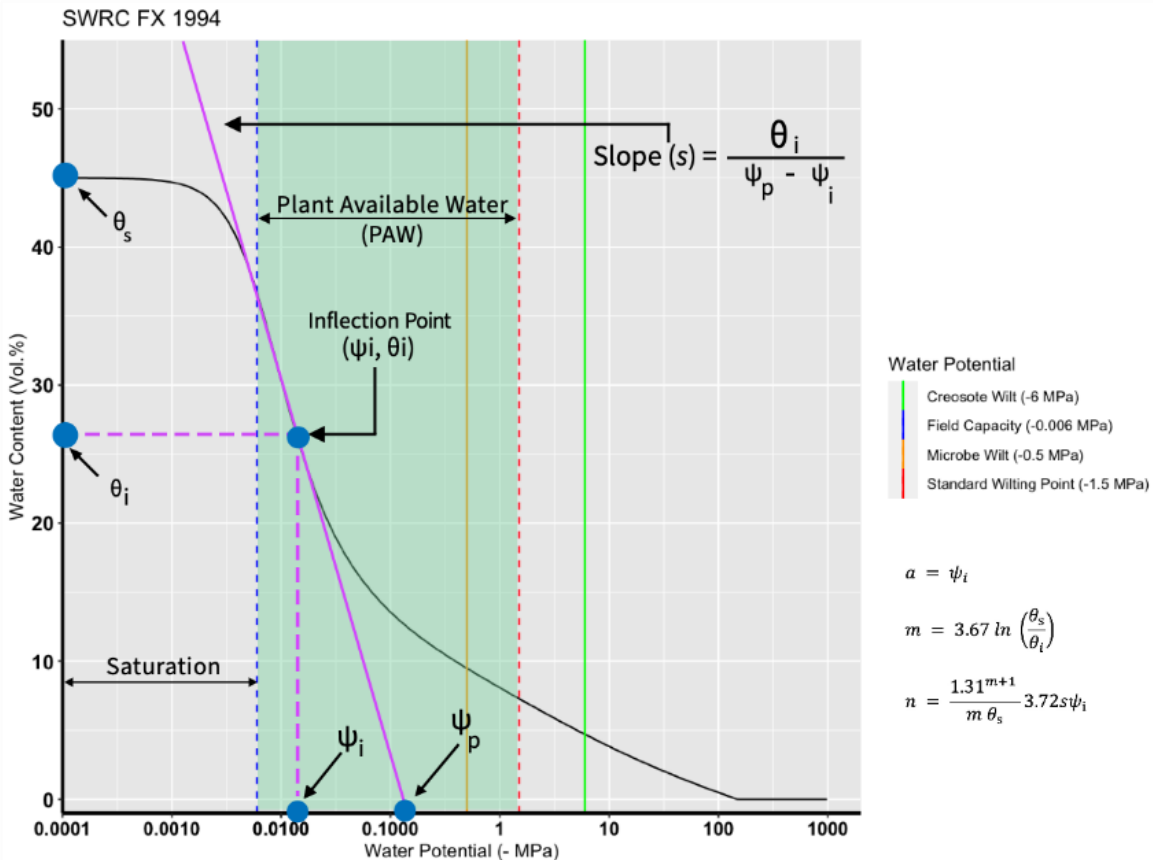

Figure 3 Soil water retention curve displaying shaping parameters (psi (i), psi (theta), psi (p), theta (i), theta(s), and slope) of the Fredlund-Xing 1994 model. Water content ranges are also shown, for saturation, field capacity, standard wilting point

SWRCs are graphical tools used to understand the amount of energy required for soils to hold and release water. These curves show the relationship between two key factors: Ψ, which is a measure of the energy state of the water in the soil measured in non-positive pressure units (MPa), and θ, which is how much water is present in the soil volumetrically, represented as a percentage. Ψ near zero indicates that the soil is at or near saturation, meaning conditions near saturation (Fig. 5). Once the soil begins to dry and θ decreases, the remaining water becomes more tightly bound to the soil particles, indicated by increasingly negative Ψ values.

SWRCs have three key phases: the saturation phase (from 0 to -0.006 MPa), the plant-available water phase (-0.006 MPa to -1.5 MPa), and the standard PWP (< -1.5 MPa). Water

contents (θ) associated with Ψ exceeding -100 MPa are not readily available to plants. In transitioning through these phases, specific parameters are identified (Fig. 3). These parameters are the saturation point, marked as θ_s, signifying the maximum amount of water that the soil can hold (which should also equal to the effective porosity). The curve's inflection point marks where Ψ_i and θ_i intersect. The slope is then calculated using the identified inflection points and the point of intersection between the tangent line and Ψ (Ψ_p) to determine the rate of change. The SWRCs were developed and analyzed using SoilView Analysis (SoilView, 2022).

2.3.1 CURVE FITTING

Using SoilView Analysis (SoilView, 2022), measured data from the Hyprop and WP4C were used for the identification of the best-fit soil hydraulic function model. The soil hydraulic function model used was the Fredlund-Xing 1994, a pedotransfer function (PTF) that determines derivatives at every point of the domain based upon measured data. The function is expressed by the following equations (Wang et al., 2016), defined as:

$$\theta(h) = \theta_{\{sX\}}(h)\, \Gamma(h), \qquad \text{Eq. 3}$$

$$\Gamma(h) = \{ln\,[e\ +\ (\alpha h)^n]\,\}^{\{-m\}}, \qquad \text{Eq. 4}$$

and

$$X(h) = 1\ - \frac{\left\{ln\left(1+\frac{h}{h_r}\right)\right\}}{\{ln(1+\frac{h_0}{h_r})\}}. \qquad \text{Eq. 5}$$

In this function, soil VWC at a pressure head, *h*, is calculated and shown as θ (*h*) in Equation 1. In the soil water saturation function, there are shaping θX (*h*) and transition Γ (*h*) functions for the SWRC. Where the shape is defined by three parameters: α, *n*, and *m*. The parameter α represents the air entry of the soil, and *n* determines the maximum slope of the

curve. Parameter *m*, ranging from 1 to 0, influences the curvature of the SWRC. For *m*, values approaching 1 suggest a smooth transition between saturated and unsaturated conditions, whereas values near 0 signify sharp transitions. The transition function X (h) (equation 3), where h_r a curve shape, and h_0 is defined as the driest observed pF. The value pF is reported on a logarithmic scale and used to describe soil water potential, calculated as pF = -log(Ψ). The pF scale covers the range from saturation at 0 pF to air-dry conditions and permanent wilting at 6 pF.

2.4 Sensor Analysis and Correction

In the JER shrubland, soil moisture sensor data ranging from 2011 to 2021 was used. A comprehensive analysis of the soil moisture data allowed for identifications and rectification of system failures, baseline shifts, and probe irregularities. By cross-referencing the adjusted sensor data with both SWRC data from corresponding depths and precise gravimetric measurements, verification and correction of the sensor data was performed to improve accuracy of the data. A linear correction equation $Y' = Y*m + c$ was applied to the data to match values with the maximum moisture content at field capacity (1.8 pF ≈ 0.063 MPa) and the minimum moisture content at air-dry conditions (6pF ≈ 1000 MPa). Through this, minimization of discrepancies over time and among different sensors was done by ensuring that each sensor's readings accurately reflected the soil moisture contents.

2.5 Conversion of Volumetric θ (VWC) Sensor Data into Matric Potential Values

Analysis of the data from Hyprop and WP4C instruments was done in order to select a soil hydraulic function through the use of the SoilView Analysis software (SoilView, 2022). This software was used to solve for a best-fit numerical model of the SWRC for each sample. The selected model was the Fredlund-Xing (FX) 1994 model, a PTF that calculates derivatives at

each point determined by the measured data. This model was selected as it performs well under varied moisture conditions, particularly in arid soils where other PTF models typically underperform (Niu et al., 2024; Ojo et al., 2022). As shown in Equation 1 (Wang et al., 2016), the FX model includes two functions: θX (*h*) and Γ(*h*). The SWRC's shape using the FX model is determined by three parameters: α is the air entry value for the soil; *n* defines the curve's maximum slope; and *m*, varying between 0 and 1, describes the curvature. Values of *m* closer to 1 produce a more gradual transition between saturated to unsaturated states, whereas values approaching 0 denote a starker transition. The transition function, X(h), includes h_r, a curve shape parameter, and h_0, the residual pressure head. For calculations and interpretations of data from soil moisture sensors and SWRC measurements, R software version 4.1.1 (R Core Team, 2021) was used. In R, the FX 1994 model was used on measured data points to develop an SWRC, which was then used to associate VWC (θ) to the soil matric potential (Ψ_m) in a more precise manner. The organisms' wilting points presented in Table 1 were used to gauge the start of the assumed physiologically activity for the organisms through the 10-year period. The amount of time in which the wilting points were exceeded was then correlated with carbon flux measurements like Gross Primary Production (GPP), Net Ecosystem Exchange (NEE), and Respiration (Reco) to explore potential for predicting ecological outcomes based on water availability.

3. RESULTS

Soil Texture Triangle

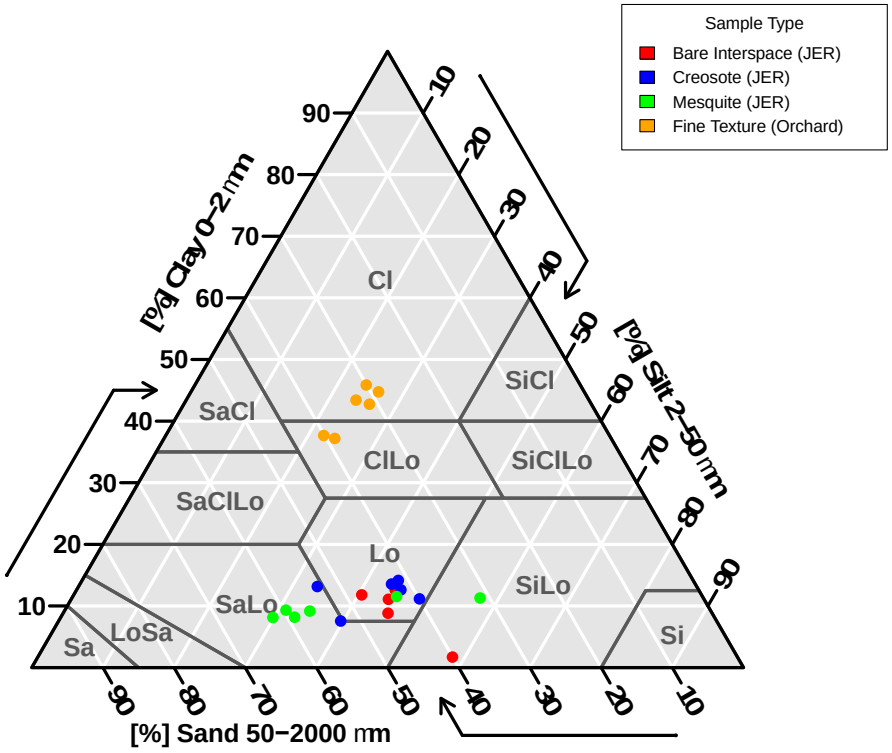

Figure 4 Soil texture triangle characterizing soils from the JER and Ivey Pecan Orchard sites. The JER samples revealed sandy loam, loam, and silty loam under bare, creosote, and mesquite coverage, respectively. At the Ivey Pecan Orchard, fine-textured clay loam

3.1 How does the shape of soil moisture retention curves vary by texture, depth, and plant cover in irrigated and shrubland dryland sites?

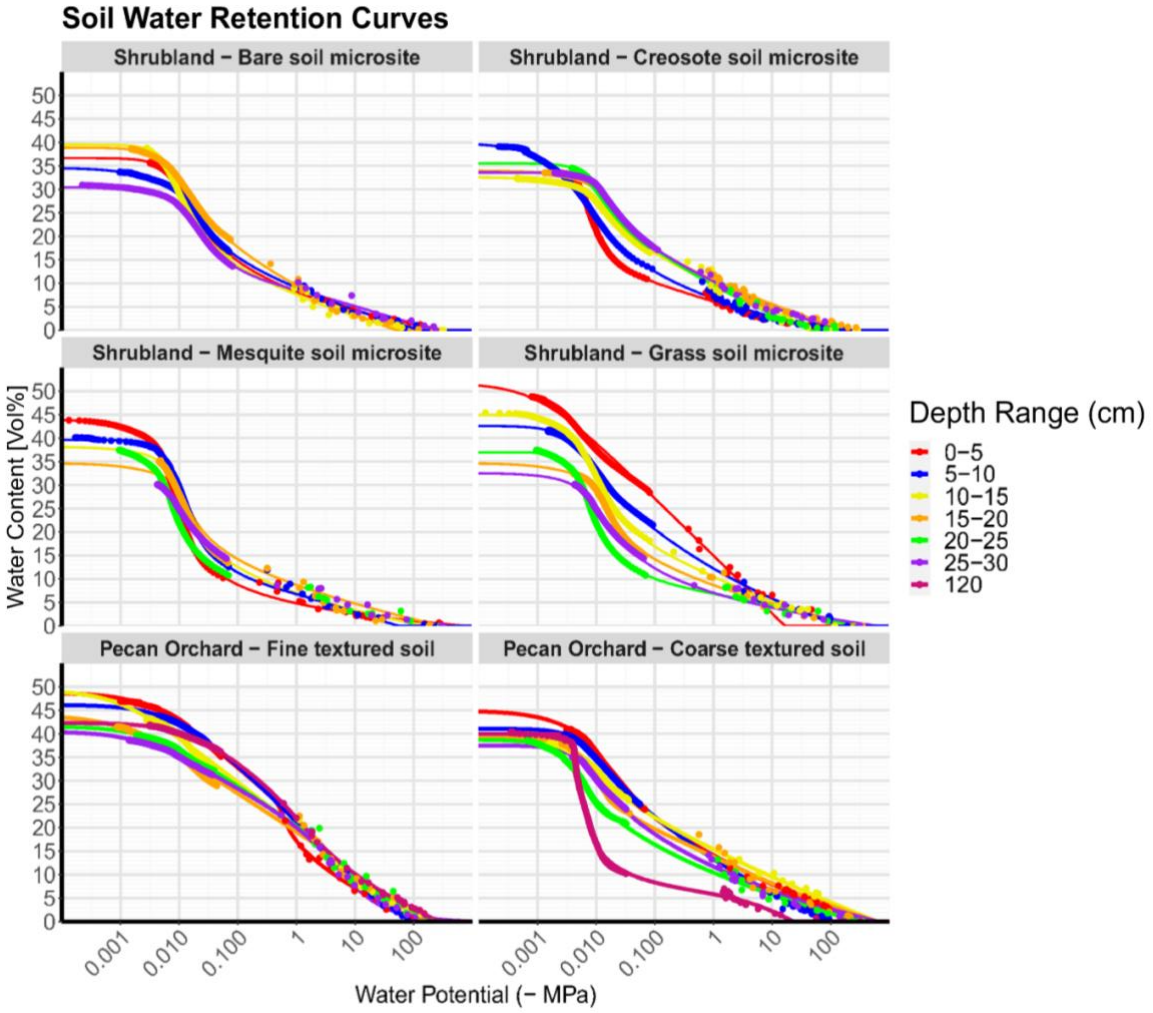

Figure 5 SWRC's for the JER site, ranging from 0-30 cm depths for soil coverage types bare, creosote, mesquite, and grass. Ivey Pecan Orchard is also shown for a depth range of 0-30 cm and 120 cm for fine and coarse textured sites.

3.1.1 Influence of Texture on SWRCs

Soil texture characterization from JER site samples included sandy loam, loam, and silty loam under bare, creosote, and mesquite coverage, respectively (Figure 4). Textural analysis showed alignment in the soil composition under creosote and bare coverage types across different depths. However, the samples below the mesquite canopy tended to have higher sand content (51.90%) (Table 2). At the Ivey Pecan Orchard, the fine-textured soil classifications were

clay and clay loam having an average composition of 42.43% clay (Table 2). Due to technical issues with the PARIO device, samples from the JER under grass coverage and Ivey pecan orchard coarse sites were unable to be processed for soil textural analysis.

SWRCs illustrate the moisture-holding capabilities of soils under varying vegetative covers and soil textures. The shape of the SWRC illustrates the decrease in soil moisture retention as soil water tension increases (Figure. 5). Curves for bare soil showed similar water losses across depth where the SWRC shape gradually narrows with increasing tension. Samples from under creosote coverage demonstrate a similar trend, indicating similar porosity of the samples across depth, with the exception of 5-10 cm showing a saturation level of 40% VWC. Also, a greater rate of water loss was seen in the upper 10 cm when compared to other SWRCs from the JER. Contrastingly, the samples under the sampled mesquite canopy displayed variation in water holding capacity, with its surface layers (0–5 cm) retaining more water than the greater depths. Samples from under grass coverage showed unique characteristics at the surface (0–5 cm) layer, showing not only a higher saturated water content, but also a better ability to retain moisture with increased water potential. This particular coverage type also showed a more distinct difference between the shallow and the deep, more so than the mesquite's trend.

Texture specifics from the Ivey Pecan orchard had shown that the fine-textured site exhibited an initial high porosity with a mild gradient decline, characteristic of clay-rich soils that exhibit high water retention as water potential tensions increase. In contrast, the coarse site displayed quick drainage, a common trait of soils with higher sand content.

Examining the soil moistures within the orchard, we observe that when the water content reaches 15% for the coarse site, the water potential is around -0.01 MPa. At the same water content, shallower soils are around -1 to -10 MPa, meaning that the 120 cm soil would allow for

much easier drainage than the shallower soil. For the fine site, the pattern is less obvious (Figure 5; Pecan Orchard Coarse textured soil).

3.1.2 Correlation Analysis of soil physical properties against SWRC shape parameters

Correlation analyses were performed using the Fredlund Xing 1994 model parameters: *m* (curvature), α (inflection point), and *n* (slope) with soil textures sand, silt, and clay (Figure 6). Additionally, data such as bulk density, saturated water content, and RMSE were also analyzed. The inflection point (α) correlated moderately with silt (r= 0.53) and strongly for clay (r = -0.67). Sand showed a weak negative relationship for parameter n (slope) r= -0.28.

In using a subset of the data to investigate patterns under coverage types, clay textures under the different coverage types showed strong correlations with α and *m* SWRC parameters. However, this was different for fine textures soils from the Ivey Pecan Orchard. While soil texture and shaping parameters yielded weak correlations, bulk density and the shaping parameters showed the strongest correlations, specifically with *n* (r= -0.96) and *m* (r= 0.63). Additionally, saturated water content correlated highest with the soil textures silt (r=-0.75) and sand (r=0.77). In comparing the shrub coverages, correlations for creosote were found to be highest for clay with the shaping parameters α and *m* ($r > 0.5$). For mesquite coverage, sand had the highest correlations with the shaping parameters α and *m*. Both shrub coverage types were shown to have weaker correlations with the *n* parameter.

Depth-specific correlation analysis yielded trends between soil textures and the SWRC shaping parameters. Throughout different depths, clay consistently maintained a strong negative correlation with α (inflection point). More specifically, clay and α at depths 5-10 cm and 15-20 cm were shown to have r = -0.63 and r = -0.8, respectively. Sand and silt textures had shown to

have more variable responses to the shaping parameters with depth, where sand and *n* (slope) had an r = 0.8 at 0-5 cm, but at 15-20 cm, the same correlation had shown r = -0.2. A trend was seen where silt was shown to have the highest correlations for α and *m*. Correlations with silt and the *n* parameter were moderate and vice versa.

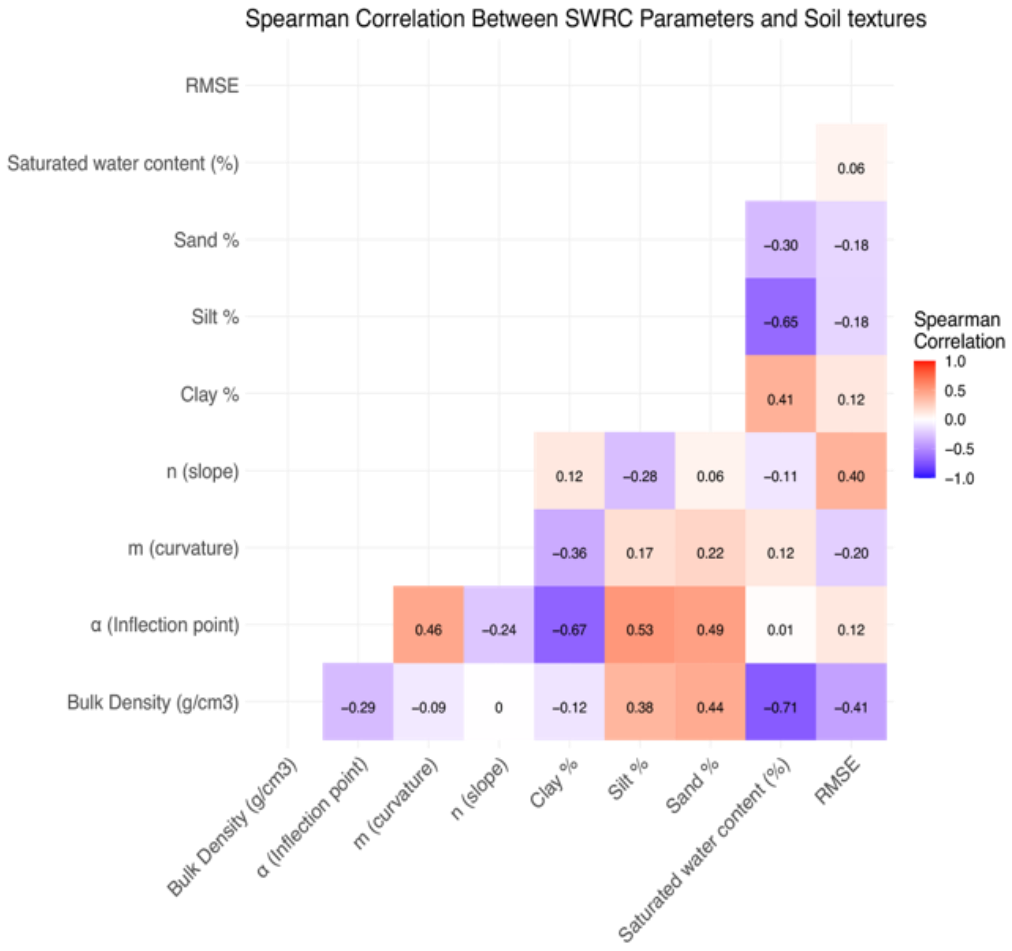

Figure 6 Correlation analysis of soil textures against Fredlund- Xing 1994 shaping parameters (α, m, and n) for creosote, mesquite, bare, and fine samples.

Table 2 The table comprises thirty-six samples, each highlighting the physical properties of soil, including bulk density and porosity, textural data such as the percentage of sand, silt, and clay, Fredlund-Xing 1994 shaping parameters (α, m and n), and initial saturated θ.

Site	Coverage/ Texture	Depth (cm)	Bulk Density (g cm^{-3})	α (Ψ_i, Inflection point)	*m* (curvature)	*n* (slope)	Clay %	Silt %	Sand %	Saturated water content (θ , %)
JER	Creosote	0-5	1.44	0.0175	0.451	4.45	7.6	39.6	52.8	33.41
	Creosote	5-10	1.38	0.0262	0.363	1.75	11.1	48.9	40	39.1
	Creosote	10-15	1.64	0.011	0.12	5.21	13.6	43.8	41.8	32.35
	Creosote	15-20	1.61	0.00891	0.175	4.08	12.6	45.6	53.3	33.54
	Creosote	20-25	1.52	0.0133	0.307	2.54	13.2	33.5	41.4	34.52
	Creosote	25-30	1.55	0.00915	0.277	2.88	14.1	44.4	45.5	33.52
JER	Mesquite	0-5	1.25	0.0158	0.503	4.09	8.1	29.8	62.1	44.18
	Mesquite	5-10	1.41	0.0131	0.669	2.44	9.3	31.1	59.6	40.14
	Mesquite	10-15	1.4	0.0135	0.331	3.82	8.2	32.9	59	35.24
	Mesquite	15-20	1.42	0.00945	0.222	5.1	9.2	34.5	56.3	32.45
	Mesquite	20-25	1.17	0.0201	0.606	2.81	11.3	57.3	31.4	37.44
	Mesquite	25-30	1.42	0.012	0.388	2.22	11.5	45.5	43	30.1
JER	Grass	0-5	1	0.00001	0.1	7.92				48.84
	Grass	5-10	1.17	0.0223	0.352	1.73				41.69
	Grass	10-15	1.13	0.0199	0.557	1.83				45.55
	Grass	15-20	1.26	0.0158	0.366	2.75				43.01
	Grass	20-25	1.11	0.0177	0.657	2.08				45.4
	Grass	25-30	1.18	0.0185	0.684	1.84				45.57
JER	Bare	0-5	1.53	0.012	0.466	2.19	8.8	45.6	45.5	35.68
	Bare	5-10	1.59	0.0075	0.203	3.59	11.1	44.6	44.3	33.66
	Bare	10-15	1.45	0.0155	0.504	2.56	12.6	44.8	42.6	38.73
	Bare	15-20	1.41	0.0135	0.429	1.89	11.8	40.5	47.7	38.59
	Bare	25-30	1.34	0.00936	0.313	1.97	1.7	58.3	40	30.88
Orchard	Fine	0-5	1.28	0.00019	0.131	10	37.2	24	38.8	47.01
	Fine	5-10	1.41	0.00003	0.552	0.89	43.4	23.9	32.7	43.75
	Fine	10-15	1.33	0.00003	0.1	3.53	40.7	23.9	35.28	43.09
	Fine	15-20	1.29	0.00003	0.1	8.29	45.9	24.1	30.1	41.47
	Fine	20-25	1.2816	0.00004	0.1	10	44.7	26.4	28.9	39.68
	Fine	25-30	1.3676	0.00002	1.42	1.215	42.7	26.1	31.2	38.65
	Fine	120	1.37988	0.00014	0.243	1.54				41.79
Orchard	Coarse	0-5	1.3688	0.0117	0.18	2.396				40.89
	Coarse	5-10	1.3604	0.0167	0.263	1.981				39.76
	Coarse	10-15	1.3398	0.0154	0.1	3.114				38.01
	Coarse	15-20	1.3404	0.0207	0.324	2.387				37.84
	Coarse	20-25	1.0794	0.0351	0.236	2.769				38.66
	Coarse	25-30	1.47996	0.0167	0.356	1.887				35.1
	Coarse	120	1.2668	0.0227	0.511	6.75				40.39

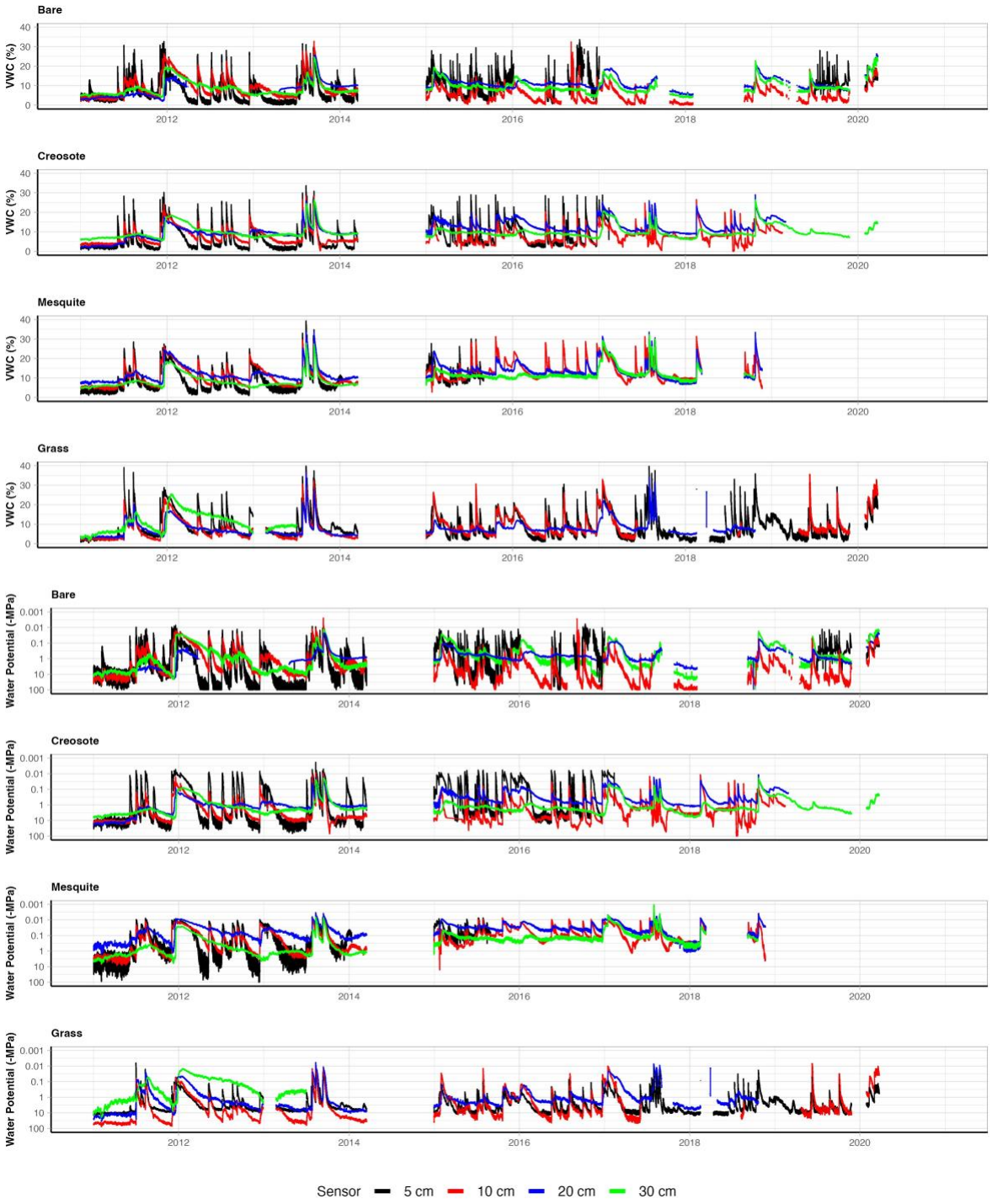

Figure 7 Graphs of sensor readings shown for various depths: 5 cm (black), 10 cm (red), 20 cm (blue), and 30 cm (green). The top four rows show the percentage of Volumetric Water Content (VWC, %), while the bottom four rows exhibits the conversion of VWC into water potential

3.2. Temporal Dynamics of Water Availability and Physiological Activity

At the JER, 16 soil moisture sensors measured VWC and Ψ data daily, every thirty minutes, from 2011 to 2021 at depths of 5, 10, 20, and 30 cm in each of 4 coverage types: creosote bush, mesquite tree, bare interspace, and grass (Figure 9). VWC trends showed significant responses to wetting events throughout the years, with scale ranges for Ψ from -100 MPa to approximately -0.01 MPa. In comparing the water potential trends against VWC, I aimed to make water availability more apparent by translating them into water potential values.

The time series for soil Ψ was created using soil moisture sensor data from the Chihuahuan desert's JER site and the SWRC fit with the FX model. Over the ten-year period, variations in soil Ψ were analyzed. The lowest difference in magnitude among sensor groups was found to be under mesquite coverage with differences in the average Ψ value for each sensor being < 2.6 MPa. In contrast, data from sensors below the creosote and below grass coverage had shown to have maximum Ψ values near -0.01 MPa, indicating conditions closer to saturation, at shallow soil depths. These results emphasize a wide range of responses observed from the different vegetation types. Under all coverage types, mesquite coverage maintained the highest Ψ values. Bare coverage experienced dry conditions at 6.6% throughout the period, reaching Ψ lower than -90 MPa. At deeper soil depths of 20 and 30 cm under bare coverage, average values of soil Ψ were calculated, resulting in -1.92 MPa and -2.86 MPa, respectively. Between 5 cm and 20 cm under bare coverage, an observed change between the sensors was about -14.33 MPa. Although not as extreme, this trend of decreasing soil Ψ magnitudes with depth was similar across all ground cover types.

3.2.1 Irrigation and Dynamics Analysis at the Ivey Pecan Orchard

Table 3 The average daily gravimetric and sensor-based soil moisture measurements at various depths, comparing daily averages of gravimetric to soil moisture sensor measurements.

Site Texture	Sensor Depth/ Type	Gravimetric AVG ($m^3\ m^{-3}$)	Soil Moisture Sensor Daily AVG ($m^3\ m^{-3}$)	Difference (%)
Coarse	30 cm	0.17	0.15	2.2
	60 cm	0.24	0.14	9.7
	90 cm	0.24	0.21	2.9
Fine	30 cm	0.30	0.28	1.1
	60 cm	0.39	0.31	7.6
	90 cm	0.41	0.22	18.9

The spatial analysis of VWC in the Ivey Pecan Orchard allowed an evaluation of the precision of soil moisture sensors by comparing them with direct gravimetric measurements converted into VWC. Averaged calculated bulk density ($g\ cm^{-3}$) measurements from each of the sites, fine and coarse, at depths of 30, 60, and 90 cm were used to convert GWC ($g\ g^{-1}$) into VWC ($m^3\ m^{-3}$). Our data collection from June 16 to 27, 2023, illuminated the contrasting moisture dynamics between coarse- and fine-textured sites around an irrigation event (Figure 9). The coarse-textured areas showed a moderate moisture increase of about 0.10 $m^3\ m^{-3}$, peaking at nearly 0.30 $m^3\ m^{-3}$. In contrast, fine-textured soils demonstrated a more substantial moisture uptake, increasing by approximately 0.28 $m^3\ m^{-3}$ (Figure 9). This contrast emphasizes the porosity differences seen between the two sites, with higher porosity in the fine-textured soils.

Further, our gravimetric measurements revealed VWC calculations with distinct moisture retention profiles within the orchard (Figure 8), particularly from 80 to 100 cm depths, which had the highest measured water content of nearly 0.7 $cm^3\ cm^{-3}$. Clay soils, in particular, showed the highest water contents, with VWC increasing from 0.37 $cm^3\ cm^{-3}$ at 0-10 cm to values

greater than 0.40 cm^3 cm^{-3} at 100 cm depth. While sandy clay soils also have higher porosity than sandy soils, their values showed minimal variation. Moisture content variation within the upper 30 cm for all types did not exceed 20%. From this data, it was revealed that the diverse water retention abilities were associated to the differing compositions of soils.

In comparing the gravimetric to the soil moisture sensor measurements (Table 3), the coarse-textured site was lowest at 30 and 90 cm, where closer agreement occurred between the measurement methods >3%. Yet, for 60 cm, the difference was about 10%. For the fine-textured site, differences between the measurement methods were highest at 90 cm, at 18.9%, suggesting a weaker correlation between the two methods at this depth. However, at 30 cm, the measurement difference was reported to be 11.1%. At 60 cm, the difference increased to 7.6%. For fine and coarse texture, the sensor readings from this location were consistently lower than

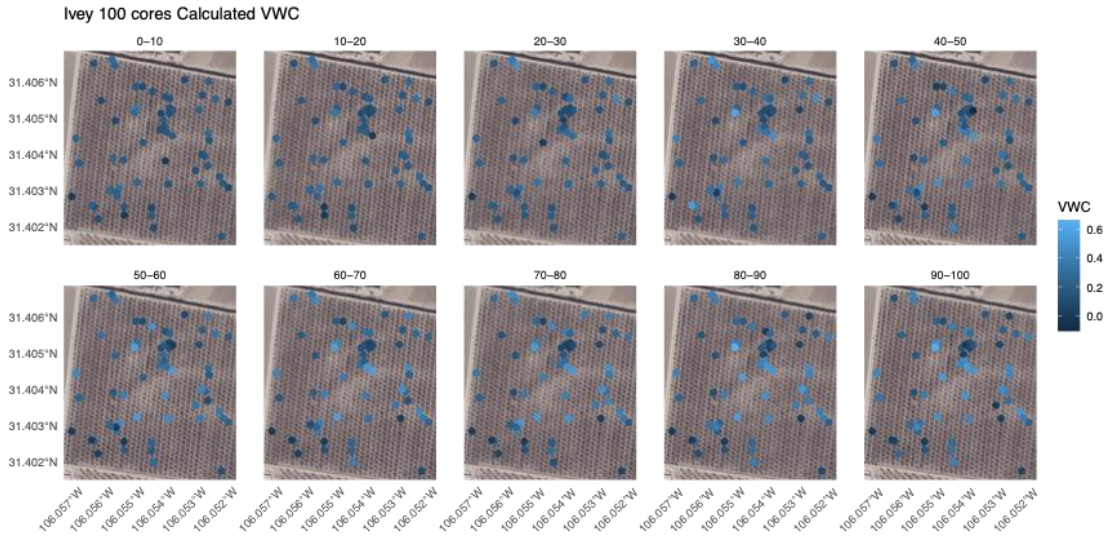

Figure 8 Spatial positioning of 100 sampling locations and corresponding VWC from the Ivey Pecan Orchard

the gravimetric measurements at all depths. Comparing the daily averages of these two measurement methods, gravimetric measurements and soil moisture sensors, better insights into potential calibration discrepancies, enhance our understanding of the sensors' performance under varied soil conditions by highlighting the differences between the measurement type values.

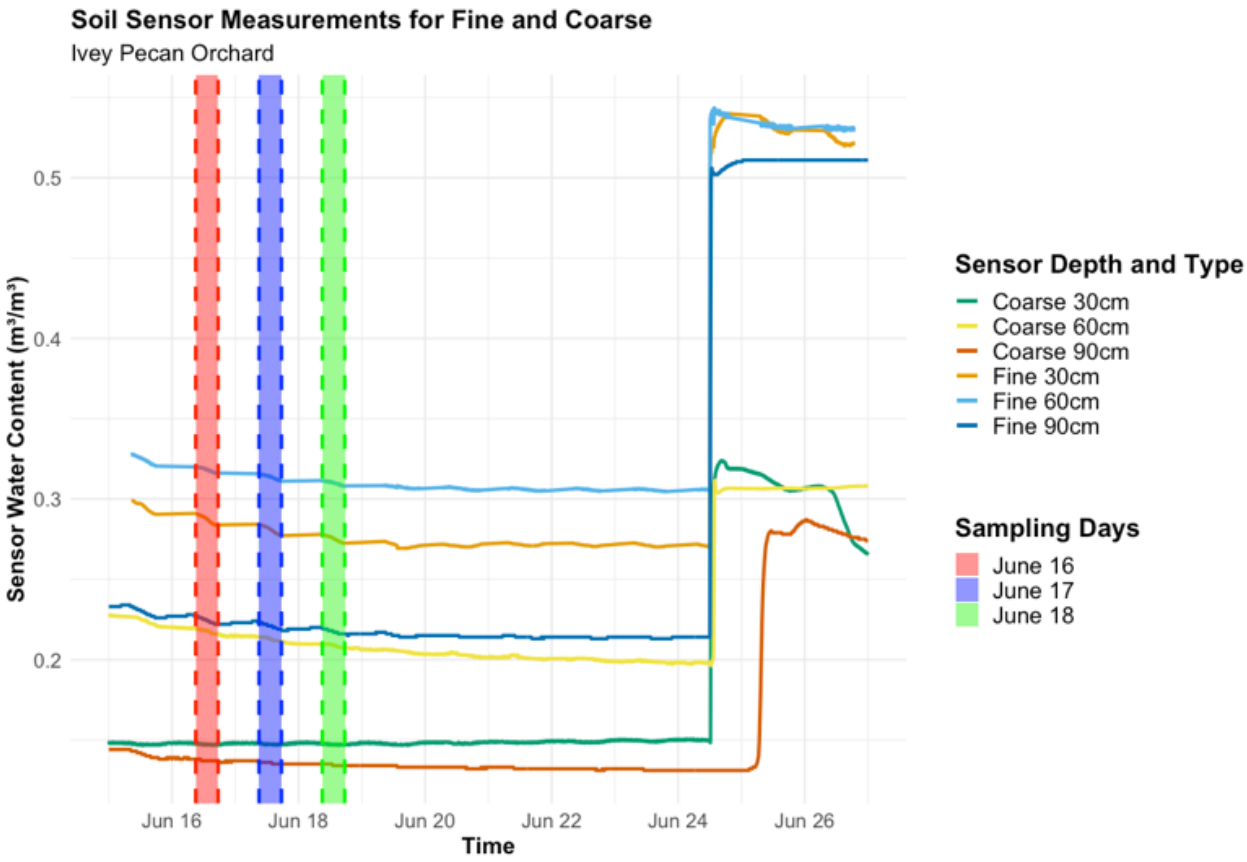

Figure 9 Soil sensor data from June 21st to June 27 displaying pre and post-irrigation events at the Ivey Pecan Orchard.

3.3. Given the plant Ψ responses of organisms in these systems such as creosote bush, mesquite, soil microbes, and biocrusts, how often do these organisms have sufficient water availability to be physiologically active over a 10-year period?

Temporal water sufficiency curves from the JER site were plotted, with indicators showing each organism's PWP as either bars to indicate a range or dashed lines to indicate fixed values (Figure 10). The results show that the 16 sensors at 4 depths × 4 plant cover types

produced differentiating responses to soil water availability. Notably, bare 10 cm and creosote 30 cm tended to plateau at certain proportions wetter than the given water potential, which was larger than 0%, unlike their counterparts. There was an abrupt increase in temporal moisture

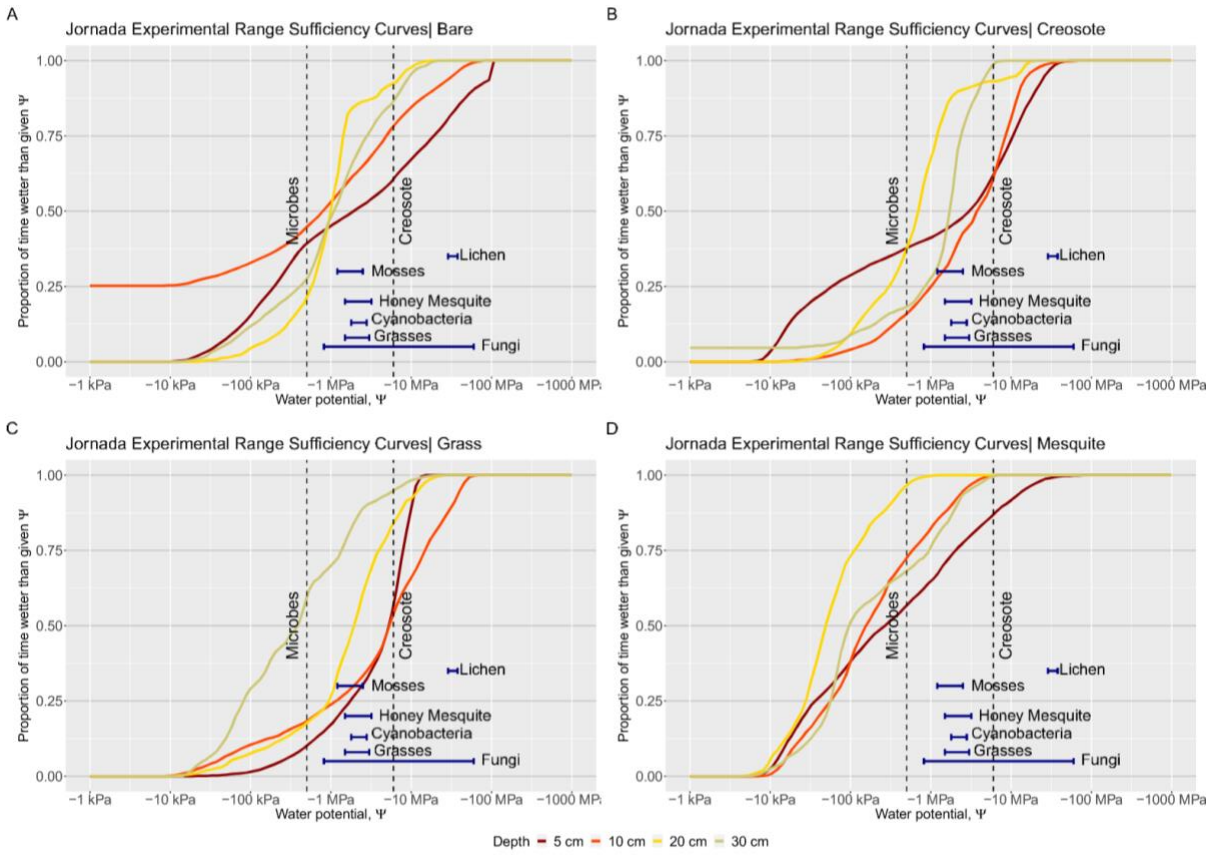

Figure 10 Percentage of time above the wilting point for organisms at each of the JER coverage types by depth. Wilting points of organisms are shown for lichen, mosses, honey mesquite, cyanobacteria, grasses, and fungi indicating a range of values in which the wilting point occurs. Microbes and Creosote wilting points are shown as dashed lines indicating fixed values for wilting points.

proportions below creosote coverage at 5 cm (Figure 10; B). The sensors under the mesquite canopy tended to maintain the highest water potentials (most available water) conditions, even at values greater than -1 MPa (Figure 10; D). These trends are worth noting because, within the other coverage types, -1 MPa tends to be the point of a sharp decrease in proportions. The only other sensor able to retain higher moisture was under grass coverage at 30 cm, which was wetter than – 80 kPa for about 25% of the time, whereas others within the same coverage types reported

less than 15% (Figure 10; C). For the PWP of creosote (-6 MPa), soils captured by several of the sensors were exceeding the sufficiency point more than 50% of the time. More variable responses were seen for mosses (-1.2 to -2.5 MPa), honey mesquite (-3.2 to -1.5 MPa), cyanobacteria (-1.8 to -2.8 MPa), and grasses (-3.0 to -1.5 MPa). The sensors in the bare and mesquite coverage locations tended to have the highest proportions of moisture conditions at the PWP.

The temporal water sufficiency curve developed for the Ivey Pecan Orchard used data collected from a 30 cm soil moisture sensor. For reasons of data completeness, dates between October 2022 and October 2023 were used. During this period, we observed a much higher proportion of time under saturated water potential conditions compared to those at JER. At -100 kPa, the curve exceeded 63%, indicating that for the observed period, the soil moisture content remained above this water potential. Significantly, the soil is infrequently found with moisture levels below this point, observed to be less than 40% of the time, suggesting that the predominant soil conditions are relatively wet, even during the non-irrigated season, which could allow for soil microbial activity year-round. Despite the instances of drier conditions, the recorded water potentials do not fall to levels that meet or exceed the wilting points of the organisms, which include pecan trees, grasses, and microbes. Instead, our data shows that water potentials exceed these values 100% of the time, which is evidenced by the fact that the sufficiency curve plateau. Soils within the orchard maintain moisture levels sufficient to preclude wilting stress for these organisms throughout the year.

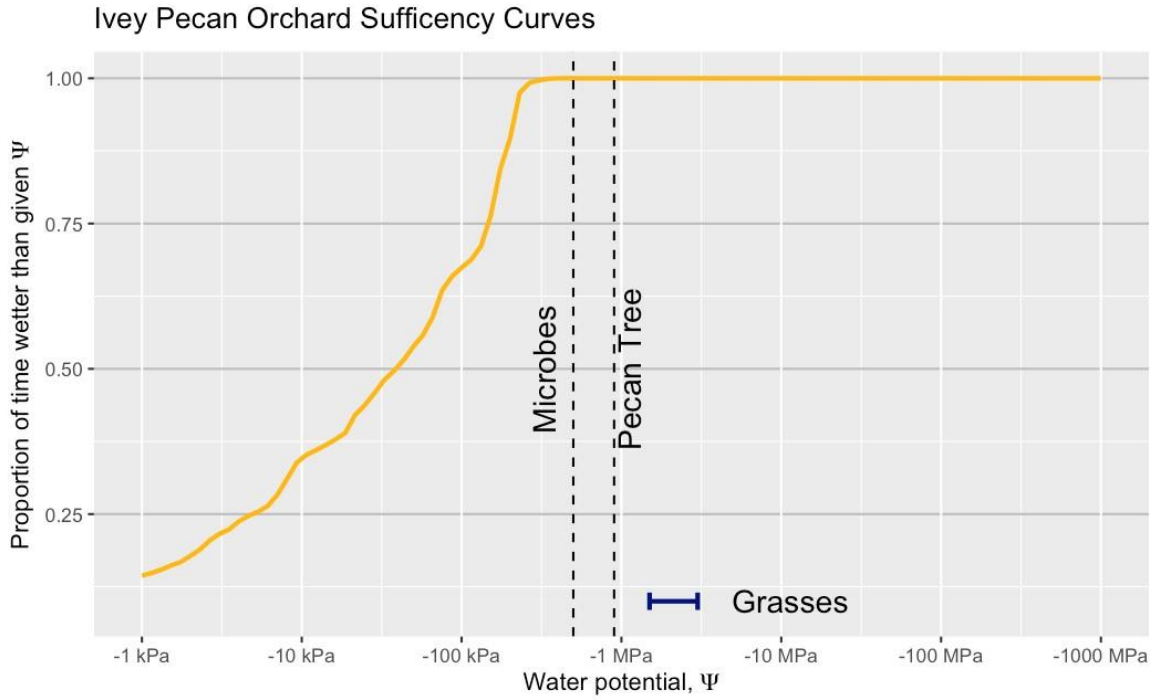

Figure 11 Percentage of time above the wilting point for organisms at each of the Ivey Pecan Orchard soil texture types at 30 cm. Wilting points of organisms are shown for grasses, indicating a range of values in which the wilting point occurs. Microbes and pecan tree wilting points are shown as dashed lines indicating fixed values for wilting points

3.4. Do these predicted intervals of physiological activities control ecosystem carbon exchange measured through eddy covariance towers?

The daily average Reco data attained from the Eddy Flux tower time series over ten years in the JER site of the Chihuahuan desert is shown (Figure 11) General trends show occurrences of extreme singular increased magnitudes. This trend shows peak values reaching yearly 2 µmol CO_2 m^{-2} s^{-1} during the years 2015, 2016, and 2021. The cyclic/seasonal trend can be seen yearly, although more pronounced for some years than others. It was also observed that descending values below 1 µmol CO_2 m^{-2} s^{-1}, the trend line shows the increased frequency of noise containing smaller magnitudes although increased variability. The relationship between carbon dynamics (NEE, GPP, Reco) and Ψ estimates was analyzed specifically under bare coverage at 10 cm depths. Three plots are presented, each containing a different dependent variable: NEE, GPP, and Reco plotted against negative log Ψ. The first scatter plot displays NEE and shows a correlation coefficient (*R*) of 0.086,

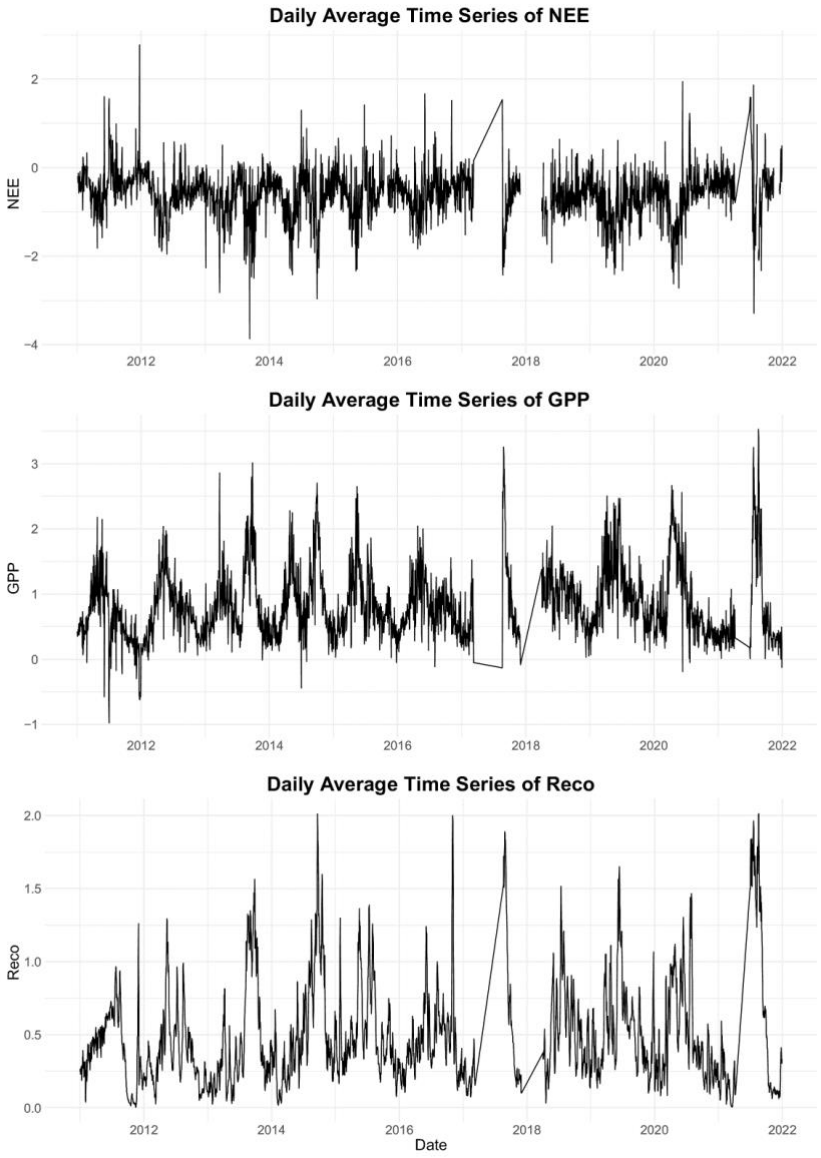

Figure 12 Time Series of Daily Average from 2011 to 2022 (A) NEE, (B) GPP, and (C) Reco.

with a p-value of 3.40e-05. This indicates a statistically significant, but weak, positive correlation between the two variables. The trend line is almost flat, suggesting only a slight increase in NEE with increasing negativity of Ψ along the x-axis. The second plot shows GPP with a correlation coefficient (*R*) of -0.031 (p-value = 0.14), indicating a non-significant and very weak negative correlation. The trend line is almost horizontal, suggesting no clear trend between GPP and Ψ values. Finally, the third plot displays Reco and shows a correlation coefficient (R) of 0.19, with a p-value of 2.20e-16.

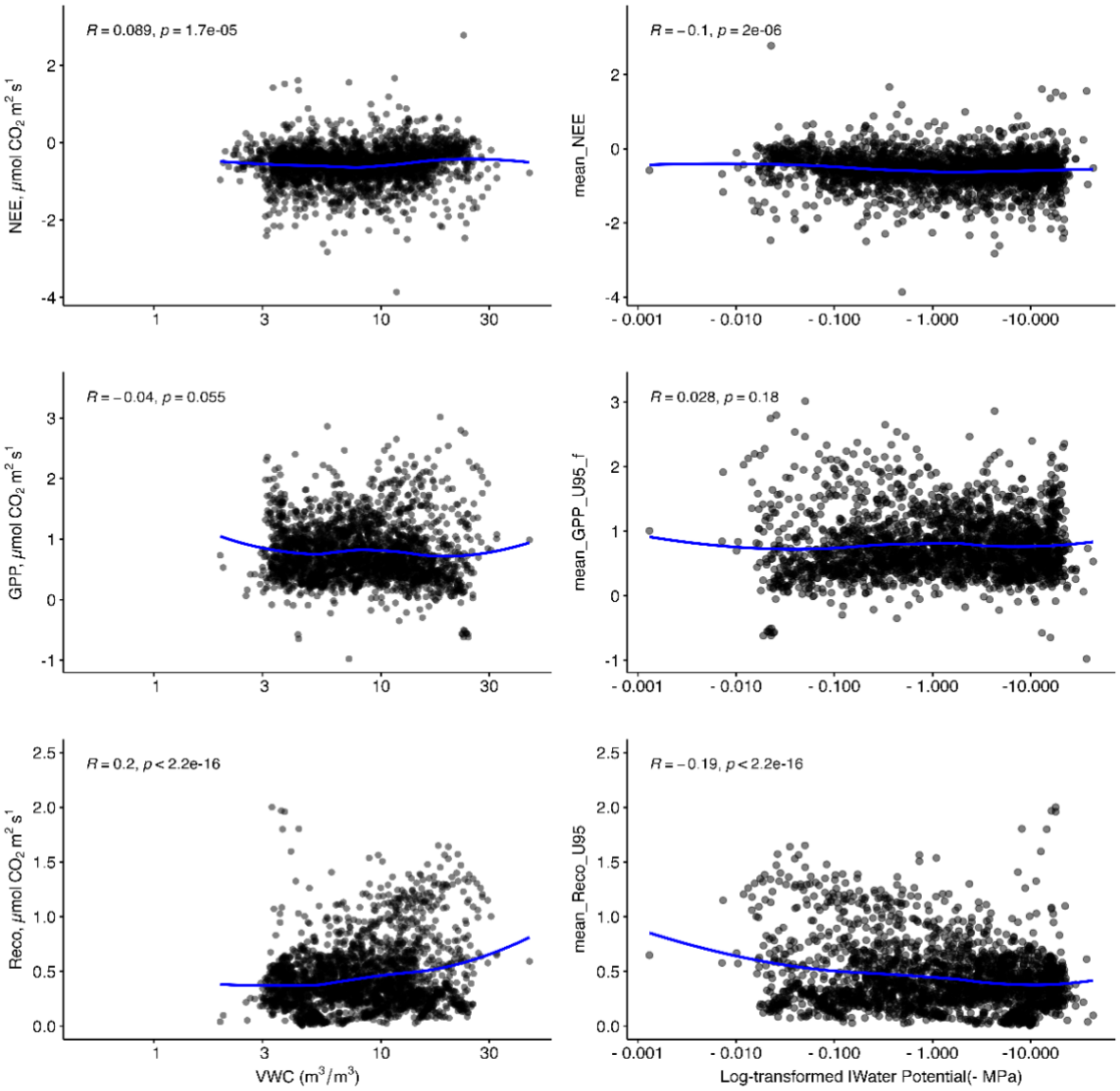

Figure 13 Negative logarithm of bare coverage data from the 10 cm depth was used. Each graph displays regression analysis results for water potentials versus NEE, GPP, and Reco.

This indicates a statistically significant, but weak, positive correlation with an upward facing trend line slope. This suggests an increase in Reco with decreasing Ψ values. Through our research, the intervals of physiological activities were predicted; in doing this, an attempt to determine if ecosystem carbon exchange is under the control of such dynamics was made. These results indicate a low ability for Ψ data to be a sole predictor for ecosystem carbon dynamics in the Chihuahuan desert JER site.

4.DISCUSSION

4.1 Soil Texture, Water Retention, and SWRC Variations

This study explored processes of the soil-plant-atmosphere continuum, identifying the interplay between soil water dynamics and carbon responses in the Chihuahuan Desert. Correlations between various soil textures—clay, silt, and sand—and the shaping parameters of the SWRC were examined, particularly focusing on the parameter α. Through the analysis, differences were seen in water retention trends across depths, as evidenced by the variations in soil moisture sensor readings when converted to Ψ. It was found that shallow soils at depths of 5 and 10 cm experienced significant increases in water loss, whereas deeper soils exhibited more temporal stability in water retention.

In conducting this correlation analysis, strong relationships among SWRC fitting functions and soil physical properties were identified. Similarly, other studies have found bulk densities and α parameter values to be negatively correlated, indicated by r of -0.732 (Jabro et al., 2022). This trend was seen for data from the fine textured soil at the Ivey Pecan orchard, where α shaping parameter and bulk density were also negatively correlated (r = -0.44). Indicating that with decreases to α, bulk densities increase. Our results showed to have stronger correlations with m (r= 0.63) and n (r = -0.95) shaping parameters when correlated with bulk densities suggesting that the SWRC slope and curvature particularly for the fine textured soils are largely influenced by BD. Additionally, studies which investigated the relationships of soil texture and BD against soil water contents had found, negative relationships for sand textures and BD while positive relationships were identified for clay (Bahmani et al., 2016). Across all of the coverage and texture types, BD with saturated water content yielded negative relationships for all but under bare coverage at the JER site. The trend of negative trends for sand was only

seen under the creosote coverage at the JER with moderate to low strengths in correlations for sand (r =-0.49), while clay was negatively correlated (r = -0.26). Through our investigation, the importance of soil physical properties on the influence of the shape of SWRCs were attempted to be understood. It is known that SWRC parameters such as α, m, and n contribute to these shapes, in conducting this correlation analysis against BD, saturated water content, and soil textures we were able to identify similar trends seen in literature. From our findings, some variables were more inclined to influence SWRC shapes for certain coverage and texture types than others. Overall, the high correlation between clay and the α shaping parameter could be due to the lower pore volumes in more compacted soils resulting in the seen inverse relationship (Chen, 2018; Jabro et al., 2022). Additionally, α may be more sensitive to variations in soil moisture as it can alter soil particle arrangements.

The contrasts seen between our findings and prior literature could be due to numerous reasons. The UNSODA database was used to access and model datasets in the referenced prior studies (Nemes et al., 2001; Cihan et al., 2009). The incongruities seen could be the result of datasets utilizing variability in measurement methods, data resolution quality, or even generalization issues that could influence the results. Additionally, the relationships between the parameters observed could also be due to the complexities of soil-water interactions indicating the necessity of incorporating additional factors into related analyses. Moreover, recognizing the significance of biological factors and biogeochemical processes influence on water retention, which manifests through changes in soil pore distribution (Saffari et al., 2019). It was observed that soil water retention varies across different depths. Our analysis of these depth trends has revealed that the relationship between soil and water is complex and variable, with inconsistent

correlations. These findings highlight the need for more comprehensive studies to better understand the intricacies of soil-water relationships.

This study underscores the critical need for precision and thoroughness in measuring soil moisture dynamics, especially highlighted by the discrepancies observed at the Ivey Pecan Orchard site. The regression between soil Ψ and carbon data attained from the eddy covariance tower was weak, indicating that the relationship between soil-plant-atmosphere relationships and the complexities of soil physical properties in the Chihuahuan Desert at this scale may be more complex. In analyzing soil moisture sensor data against VWC measurements, discrepancies at the Ivey Pecan Orchard site indicated accuracy concerns for soil moisture sensor data when compared. The call for comprehensive sampling to better comprehend spatial variability and biotic processes in soil moisture dynamics becomes particularly pertinent in complex ecosystems like the Chihuahuan Desert (Knapp et al., 1993; Cale et al., 1989; Sellers et al., 1988; Avissar et al., 1991; Schimel et al., 1991). Ultimately, our research paves the way for future studies to examine these complexities, promoting a greater comprehension of soil-water relationships that are vital for understanding natural and agricultural systems.

4.2 Influences of Biological Factors and Environmental Conditions

Soil is the crucial medium by which organisms absorb water, playing an essential role in water retention and the health of ecosystems (Hosseini et al., 2016). Traditionally, a water potential of -1.5 MPa has been recognized as the PWP, the critical threshold below which plants fail to meet their water needs. A review of literature showed variations in PWP across different species, especially in dryland areas. Through the literature, species of fungi able to reach water

potentials of -60 MPa, as well as common plant species within the Chihuahuan desert, such as Creosote (-6 MPa) and mesquite (- 3.2 MPa), were identified.

Our study revealed that dryland soils exhibit varied responses to water content which result in variable water availability for organisms, indicating the complexity of plant-soil water interactions. Such complexities suggest that the conventional -1.5 MPa threshold is only applicable in some cases, particularly in dryland contexts. Earlier studies have also highlighted this, stating that plant types can maintain and uptake water at potentials significantly even lower than -1.5 MPa, observing ranges between -2.0 to -5.0 MPa (Sauer et al., 1984). In focusing on water potential (Ψ), inconsistencies have been uncovered with the widely accepted PWP value. Although research on PWP in dryland species exists, further investigation is required to interpret possible shifts or variances in PWP under changing conditions, enhancing our understanding of plant responses to environmental stressors.

4.3 Sensor Accuracy, Calibration, and Plant-Water Relations

Moisture inputs and losses, primarily through evapotranspiration, are crucial in driving soil Ψ changes, with semi-arid regions showing soil water dynamics influenced by storage-dominated sites (Lauenroth et al., 2009). These sites experience moisture accumulation during fall, winter, and spring, leading to consistent water availability in spring and early summer, especially in deeper soil layers (Schlaepfer et al., 2011). A decade-long analysis (2011-2021) in the Chihuahuan desert examining VWC and calculated Ψ across various depths and vegetation types revealed that wetting events often led to VWC levels above 25% below 10 cm depth annually across all vegetation types. Seasonal variations in Ψ were clear, showing different trends throughout the year, with shallower depths experiencing greater temporal variability (Yue et al., 2018). Despite the variability in VWC measurements, Ψ magnitudes for wetting events

were similar, indicating greater stability in soil moisture for Ψ overall. Surface soil layers and those near vegetation, influenced by rainfall and evapotranspiration, reacted more compared to deeper layers (Rezaur et al., 2002). Shallow soils showed oscillating Ψ trends, with extreme conditions more common, while deeper layers exhibited increased temporal stability. At depths of 20 and 30 cm, Ψ were consistently higher, with a notable difference observed in areas devoid of vegetation. August data showed temporally stable soil Ψ at 30 cm depth, persisting after wet-dry cycles (Wendroth et al., 1999). Research from January to March indicated increases in soil matric potentials, surpassing the PWP at up to 20 cm depths (Bravo et al., 2020), highlighting challenges in maintaining measurement consistency across different systems and conditions (Sala et al., 1981). VWC measurements were more sensitive to minor changes under wet conditions, becoming less sensitive under drier conditions. This comprehensive analysis underscores the complex dynamics of soil moisture and the influence of depth, vegetation, and seasonal variations on soil Ψ, crucial for understanding water availability in semi-arid ecosystems.

4.3.1 IVEY PECAN ORCHARD

In extending our analysis to the Ivey Pecan Orchard, spatial analysis of gravimetric measurements revealed trends in moisture distribution patterns. Comparisons of irrigation responses of different soil textures within the orchard were also made, resulting in fine-textured soils exhibiting greater moisture post-irrigation compared to coarse-textured soils. This highlights the impact of soil texture on water retention capabilities. Accurate moisture monitoring for effective water management in agricultural settings is crucial, and highlighted the effectiveness of irrigation on soil moisture across various depths and soil types. Our analysis found spatial patterns in VWC, pinpointing areas within the central regions of the orchard that

retain more moisture, particularly with increased depth. This observation was supported by the fine-textured soils at 30 and 90 cm absorbing more moisture post irrigation than their coarse-textured counterparts, highlighting the differences of soil texture on water retention. A study demonstrated that irrigation significantly enhances soil water retention across various depths and soil types, with matric potentials showing that conditions remained saturated down to 75 cm throughout the summer months (Engelhardt et al., 2009). Previous studies have shown that the soil θ values were generally lower than the GWC values for soil moisture sensors (Groves & Rose, 2004; Mead et al., 1995). Employing manufacturer's calibration equations for soil moisture sensors underestimated actual θ by approximately 1.2 times at three different θ (Haberland et al., 2014). An FDR sensor (EnviroSCAN by Sentek) was highly sensitive to changes in the VWC in the dry and intermediate ranges. In contrast, it was relatively insensitive to changes in the VWC in wet to very wet soils (Roberti et al., 2018). In addition, the FDR sensor had two major limitations when measuring the VWC where it failed to measure VWC > 0.40 cm^3 cm^{-3}accurately, and its sensitivity decreased as the VWC increased (Jia et al., 2020). GWC was significantly lower at 0-10 cm (Bogunović et al., 2016), and the average θ in the soil profile (0–90 cm) in 1998 showed a sharp increase in soil θ after the irrigation event for alfalfa. Even though the trends are similar, the actual sensor readings differed by 0.15 m^3 m^{-3} of θ at any given measurement date. The chance of obtaining accurate soil water measurements without site-specific calibration is poor (Leib et al., 2003). A previous study of temperature calibration of 5TM soil moisture sensors found that θ was underestimated under high temperature and high-θ conditions and was overestimated in low θ environments (Schwartz et al., 2019). 5TM sensor readings were calibrated with the "true" values of the gravimetric method. After the calibration of LCM, θ improved accuracy by 3.4% (Li et al., 2022).

4.4 Implications for Carbon Dynamics and Ecosystem Research

The linkage between carbon dynamics and Ψ in ecosystems highlighted the complexities between physiological activities and carbon exchange. From the JER site in the Chihuahuan Desert, during 2015, 2016, and 2021, daily average respiration (Reco) data attained from the Eddy Flux tower showed yearly spikes in CO_2 emissions, peaking at 2 µmol CO_2 m^{-2} s^{-1}. The cyclic patterns with varying degrees of prominence through the years displayed fluctuations. The variability in the data increased in frequency, particularly when values decreased below 1 µmol CO_2 m^{-2} s^{-1}.

When the relationship between carbon (NEE, GPP, Reco) and Ψ was examined at a 10 cm depth below bare coverage, the analysis revealed a weak positive statistically significant correlation between NEE and Ψ, with a correlation coefficient $r = 0.086$ and a p-value = 3.40e-05 and Reco displayed a weak positive correlation ($r = 0.19$, p-value < 0.01) with Ψ, showing a slight increase in Reco as Ψ decreases. Prior research has focused on the response of grassland ecosystems to rising CO_2 levels, including factors such as leaf photosynthesis, Ψ, and soil-water depletion to address sensitivities in water-limited ecosystems. From their observations, they were able to ascertain that complex interactions of CO_2 concentrations directly influence water dynamics, affecting carbon exchange processes within ecosystems. Soil respiration patterns were found to closely relate to soil Ψ, especially at the 10 cm depth, highlighting a significant relationship with soil Ψ following precipitation events and highlighting the interconnectedness of water dynamics, CO_2 levels, and carbon exchange processes (Polley et al., 2002). Additionally, respiration decreases with decreasing Ψ in pasture/forest soils were found to occur between wetting cycles (Setia et al., 2013; Davidson et al., 2000). This linear model lacked the specific considerations needed to model carbon within a realistic scope. This portion of the research

could have benefited from the inclusion and consideration of not only soil moisture contents but also nutrient contributions, seasonality, organic matter contributions in soils, and night and day cycles, which influence stomata activations. Due to the exclusion of these variables, we were not able to identify strong correlations between the soil moisture data and NEE, RECO, or GPP. Although our study delved into the carbon dynamics and water relationships in drylands, there is a pressing need for broader-scale modeling approaches that the scope of our research was unable to address.

5. CONCLUSION

In this study, identification of patterns related to the soil physical properties, such as texture, depth, and under coverage types lent support to the underlying precept that soil physical parameters impact the SWRC shapes. The main results of this thesis indicate that there are low correlations between soil textures (sand, silt, and clay) and the shaping parameter α of the SWRC compared to the influence of the other shaping parameters. As seen in our data, this relationship is common. It occurs across different land cover types and soil depths, indicating that certain shaping parameters, when combined with specific soil textures, are more influential in determining the SWRC's structure.

When analyzing temporal dynamics in the Chihuahuan Desert through the identification of dryland PWP and assessing the percentage of time these values were exceeded, it was found that the sensors at 4 depths underneath the mesquite canopy showed the highest rate of exceeding the PWP overall. While the data only come from one shrub, they suggest the intriguing possibility that the deep-rooted mesquite shrubs keep shallow layers wetter through hydraulic redistribution (Ehleringer et al., 1999; Lee et al., 2021). Although it was expected that the shrub species would behave more similarly, this was not the case collectively. Below coverage for shrub species, water was maintained more than 50% of the time above the lowest wilting point, that of creosote (-6 MPa), indicating that water is available for a considerable portion of the year.

Our spatial analysis of soil moisture conducted at the Ivey Pecan Orchard allowed for the identification of any misrepresentations for broader areas of interest through the use of sensor data. The gravimetric measurements indicated trends of increased moisture with depth, while soil sensors underestimated moisture at the coarse site and overestimated it at the fine site. Numerous

mechanical and calibration-related issues could arise, potentially resulting in biased data that may require data correction.

Our investigations showed for Reco (Ecosystem Respiration), Ψ did show a slightly higher R-squared, only explaining 20% of the variance. While the linear model used for this analysis was unsophisticated, it suggests a need for a more comprehensive model-based analysis could be useful for a better understanding of the relationship between water potential and tower fluxes in drylands. Additionally, other factors could influence soil moisture that were not considered throughout this study. Incorporation of these influences could provide a more comprehensive understanding of the mechanisms controlling soil plant atmosphere dynamics in dryland environments. This information could be more relevant to the broader understanding of the role of water availability on land carbon dynamics. In our investigation, developments of temporal soil water sufficiency curves and their ability to indicate water availability under coverage types successfully contribute to the broader understanding of water availability in drylands, providing a solid foundation for future studies.

6. REFERENCES

Airori, A. J., Baker, T. J., & Turk, J. K. (2022). The impact of sampling methodology on soil bulk density measurement by the clod method. *Communications in Soil Science and Plant Analysis*, *53*(3), 317–326. https://doi.org/10.1080/00103624.2021.1993887

Antunes, C., Díaz Barradas, M. C., Zunzunegui, M., Vieira, S., Pereira, Â., Anjos, A., Correia, O., Pereira, M. J., & Máguas, C. (2018a). Contrasting plant water-use responses to groundwater depth in coastal dune ecosystems. *Functional Ecology*, *32*(8), 1931–1943. https://doi.org/10.1111/1365-2435.13110

Archer, J. R., & Smith, P. D. (1972). The relation between bulk density, available water capacity, and air capacity of soils. *Journal of Soil Science*, *23*(4), 475–480. https://doi.org/10.1111/j.1365-2389.1972.tb01678.x

Arvidsson, J. (1998). Influence of soil texture and organic matter content on bulk density, air content, compression index and crop yield in field and laboratory compression experiments. *Soil and Tillage Research*, *49*(1–2), 159–170. https://doi.org/10.1016/S0167-1987(98)00164-0

Bahmani, O., & Palangi, S. (2016). Evaluation of pedotransfer functions for estimating the soil water retention points. *Eurasian Soil Science*, *49*(6), 652–660. https://doi.org/10.1134/S1064229316060028

Bahmani, O., Palangi, S. Evaluation of pedotransfer functions for estimating the soil water retention points. Eurasian Soil Sc. 49, 652–660 (2016). https://doi.org/10.1134/S1064229316060028

Baruch, Z., & Bilbao, B. (1999a). Effects of fire and defoliation on the life history of native and invader C 4 grasses in a Neotropical savanna. *Oecologia*, *119*(4), 510–520. https://doi.org/10.1007/s004420050814

Bilskie, J. (ND). Soil water Status: Content and potential – Campbell Sci. Retrieved February 13, 2023. https://s.campbellsci.com/documents/us/technical-papers/soilh20c.pdf

Brock, T. D. (1975). Effect of water potential on a *microcoleus* (Cyanophyceae) from a desert crust [1]. *Journal of Phycology*, *11*(3), 316–320. https://doi.org/10.1111/j.1529-8817.1975.tb02786.x

Browning, D. M., Duniway, M. C., Laliberte, A. S., & Rango, A. (2012). Hierarchical analysis of vegetation dynamics over 71 years: Soil–rainfall interactions in a Chihuahuan Desert ecosystem. *Ecological Applications*, *22*(3), 909–926. https://doi.org/10.1890/11-1193.1

Buljak, V., & Ranzi, G. (2021). Calibration of constitutive models. Constitutive Modeling of Engineering Materials, 43-53. https://doi.org/10.1016/B978-0-12-814696-5.00007-1

Cantón, Y., Chamizo, S., Rodriguez-Caballero, E., Lázaro, R., Roncero-Ramos, B., Román, J. R., & Solé-Benet, A. (2020). Water regulation in cyanobacterial biocrusts from drylands: Negative impacts of anthropogenic disturbance. *Water*, *12*(3), 720. https://doi.org/10.3390/w12030720

Chaudhari, P.R., Ahire, D.V., Ahire, V.D., Chkravarty, M., & Maity, S. (2013). Soil Bulk Densityas related to Soil Texture , Organic Matter Content and available total Nutrients of Coimbatore Soil.

Chen, J., Cui, H.-Y., Jia, B., Gang, S., Li, Y., Li, F.-C., Ming Mou, X., & Li, X. G. (2022). Soil sampling depth matters in assessing the impact of shrubification on soil organic carbon storage in grazed alpine meadows. *Geoderma*, *426*, 116119. https://doi.org/10.1016/j.geoderma.2022.116119

Chen, L., & Dick, W. (2011). Gypsum as an agricultural amendment. [Columbus, OH]. Ohio State University Press.

Chen, Y. (2018). Soil–water retention curves derived as a function of soil dry density. GeoHazards, 1(1), 3-19.

Chowdhury, N., Marschner, P., & Burns, R. G. (2011b). Soil microbial activity and community composition: Impact of changes in matric and osmotic potential. *Soil Biology and Biochemistry*, *43*(6), 1229–1236. https://doi.org/10.1016/j.soilbio.2011.02.012

Cihan, A., Tyner, J. S., & Perfect, E. (2009). Predicting relative permeability from water retention: A direct approach based on fractal geometry. Water Resources Research, 45(4). https://doi.org/10.1029/2008WR007038

Cook, R. J., Papendick, R. I., & Griffin, D. M. (1972). Growth of two root-rot fungi as affected by osmotic and matric water potentials. *Soil Science Society of America Journal*, *36*(1), 78–82. https://doi.org/10.2136/sssaj1972.03615995003600010018x

Crawford, J. W., Matsui, N., & Young, I. M. (1995). The relation between the moisture-release curve and the structure of soil. *European Journal of Soil Science*, *46*(3), 369–375. https://doi.org/10.1111/j.1365-2389.1995.tb01333.x

Crowley, B., Bataille, C. P., Britton, K., Miller, J. H., & Wooller, M. (2022, February 18). *A Golden Age for Strontium Isotope Research? Current Advances in Paleoecological and Archaeological Research*. Frontiers Media SA.

Crump, W. B. (1913). Notes on water-content and the wilting-point. *The Journal of Ecology*, *1*(2), 96. https://doi.org/10.2307/2255669

D'Odorico, P., & Bhattachan, A. (2012). Hydrologic variability in dryland regions: Impacts on ecosystem dynamics and food security. *Philosophical Transactions of the Royal Society B: Biological Sciences*, *367*(1606), 3145–3157. https://doi.org/10.1098/rstb.2012.0016

Daba, A. W., & Qureshi, A. S. (2021b). Review of soil salinity and sodicity challenges to crop production in the lowland irrigated areas of ethiopia and its management strategies. *Land*, *10*(12), 1377. https://doi.org/10.3390/land10121377

Darrouzet-Nardi, A., Reed, S. C., Grote, E. E., & Belnap, J. (2015). Observations of net soil exchange of CO_2 in a dryland show experimental warming increases carbon losses in biocrust soils. *Biogeochemistry*, *126*(3), 363–378. https://www.jstor.org/stable/24711606

Dawson, T. E., Hahm, W. J., & Crutchfield-Peters, K. (2020a). Digging deeper: What the critical zone perspective adds to the study of plant ecophysiology. *New Phytologist*, *226*(3), 666–671. https://doi.org/10.1111/nph.16410

De Oliveira, R. A., Ramos, M. M., & De Aquino, L. A. (2015a). Irrigation management. In *Sugarcane* (pp. 161–183). Elsevier. https://doi.org/10.1016/B978-0-12-802239-9.00008-6

Domínguez-Niño, J. M., Arbat, G., Raij-Hoffman, I., Kisekka, I., Girona, J., & Casadesús, J. (2020). Parameterization of soil hydraulic parameters for hydrus-3d simulation of soil water dynamics in a drip-irrigated orchard. *Water*, *12*(7), 1858. https://doi.org/10.3390/w12071858

Durner, W., & Iden, S. C. (2021b). The improved integral suspension pressure method (Isp+) for precise particle size analysis of soil and sedimentary materials. *Soil and Tillage Research*, *213*, 105086. https://doi.org/10.1016/j.still.2021.105086

Dusek, J., Dohnal, M., Vogel, T., Marx, A., & Barth, J. A. C. (2019b). Modelling multiseasonal preferential transport of dissolved organic carbon in a shallow forest soil: Equilibrium versus kinetic sorption. *Hydrological Processes*, *33*(22), 2898–2917. https://doi.org/10.1002/hyp.13536

Dusenge, M. E., Duarte, A. G., & Way, D. A. (2019). Plant carbon metabolism and climate change: Elevated CO_2 and temperature impacts on photosynthesis, photorespiration and respiration. *New Phytologist*, *221*(1), 32–49. https://doi.org/10.1111/nph.15283

Easter, S. J. (1973). *Water relationships of honey mesquite (Prosopis glandulosa Torr. var. glandulosa)* ([Doctoral Dissertation]. Texas Tech University).

Ehleringer, J. R., Schwinning, S., & Gebauer, R. (1999). Water use in arid land ecosystems. *Physiological Plant Ecology*, 347.

Emerson, W. (1995b). Water-retention, organic-C and soil texture. *Soil Research*, *33*(2), 241. https://doi.org/10.1071/SR9950241

Engelhardt, S., Matyssek, R., & Huwe, B. (2009b). Complexity and information propagation in hydrological time series of mountain forest catchments. *European*

Journal of Forest Research, *128*(6), 621–631. https://doi.org/10.1007/s10342-009-0306-2

English, N. B., Weltzin, J. F., Fravolini, A., Thomas, L., & Williams, D. G. (2005). The influence of soil texture and vegetation on soil moisture under rainout shelters in a semi-desert grassland. *Journal of Arid Environments*, *63*(1), 324–343. https://doi.org/10.1016/j.jaridenv.2005.03.013

Er Yue & John N. Veenstra. (2018a). Prediction of active zone depth in oklahoma using soil matric suction. *Journal of GeoEngineering*, *13*(1). https://doi.org/10.6310/jog.201803_13(1).3

Evett, S. R., Schwartz, R. C., Casanova, J. J., & Heng, L. K. (2012). Soil water sensing for water balance, ET and WUE. *Agricultural Water Management*, *104*, 1–9. https://doi.org/10.1016/j.agwat.2011.12.002

Faust, A. E., Ferré, T. P. A., Schaap, M. G., & Hinnell, A. C. (2006). Can basin-scale recharge be estimated reasonably with water-balance models? *Vadose Zone Journal*, *5*(3), 850–855. https://doi.org/10.2136/vzj2005.0109

Fernandez-Illescas, C. P., Porporato, A., Laio, F., & Rodriguez-Iturbe, I. (2001). The ecohydrological role of soil texture in a water-limited ecosystem. *Water Resources Research*, *37*(12), 2863–2872. https://doi.org/10.1029/2000WR000121

Flint, A. L., Flint, L. E., Hevesi, J. A., & Blainey, J. B. (2004). Fundamental concepts of recharge in the desert southwest: A regional modeling perspective. In J. F. Hogan, F. M. Phillips, & B. R. Scanlon (Eds.), *Water Science and Application* (Vol. 9, pp. 159–184). American Geophysical Union. https://doi.org/10.1029/009WSA10

Fredlund, Delwyn G., and Anqing Xing. "Equations for the soil-water characteristic curve." Canadian geotechnical journal 31.4 (1994): 521-532.

Garcia-Pichel, F., & Sala, O. (2022b). *Expanding the pulse-reserve paradigm to microorganisms on the basis of differential reserve management strategies*. https://doi.org/10.1101/2022.02.24.481838

Garg, A., Bordoloi, S., Ganesan, S. P., Sekharan, S., & Sahoo, L. (2020b). A relook into plant wilting: Observational evidence based on unsaturated soil–plant-photosynthesis interaction. *Scientific Reports*, *10*(1), 22064. https://doi.org/10.1038/s41598-020-78893-z

Giménez, C., Gallardo, M., & Thompson, R. B. (2013b). Plant–water relations. In *Reference Module in Earth Systems and Environmental Sciences* (p. B978012409548905257X). Elsevier. https://doi.org/10.1016/B978-0-12-409548-9.05257-X

Golluscio, R. A., Escalada, V. S., & Pérez, J. (2009b). Minimal plant responsiveness to summer water pulses: Ecophysiological constraints of three species of semiarid

patagonia. *Rangeland Ecology & Management*, *62*(2), 171–178. https://doi.org/10.2111/08-196.1

Green, T. G. A., & Proctor, M. C. F. (2016b). Physiology of photosynthetic organisms within biological soil crusts: Their adaptation, flexibility, and plasticity. In B. Weber, B. Büdel, & J. Belnap (Eds.), *Biological Soil Crusts: An Organizing Principle in Drylands* (Vol. 226, pp. 347–381). Springer International Publishing. https://doi.org/10.1007/978-3-319-30214-0_18

Green, T. G. A., Pintado, A., Raggio, J., & Sancho, L. G. (2018b). The lifestyle of lichens in soil crusts. *The Lichenologist*, *50*(3), 397–410. https://doi.org/10.1017/S0024282918000130

Griffiths, R. I., Whiteley, A. S., O'Donnell, A. G., & Bailey, M. J. (2003a). Physiological and community responses of establishedgrassland bacterial populations to waterstress. *Applied and Environmental Microbiology*, *69*(12), 6961–6968. https://doi.org/10.1128/AEM.69.12.6961-6968.2003

Guo, J. S., & Ogle, K. (2019b). Antecedent soil water content and vapor pressure deficit interactively control water potential in *Larrea tridentata*. *New Phytologist*, *221*(1), 218–232. https://doi.org/10.1111/nph.15374

Haas, R. H., & Dodd, J. D. (1972b). Water-stress patterns in honey mesquite. *Ecology*, *53*(4), 674–680. https://doi.org/10.2307/1934782

Hadas, A. (2005a). Germination and seedling establishment. In *Encyclopedia of Soils in the Environment* (pp. 130–137). Elsevier. https://doi.org/10.1016/B0-12-348530-4/00149-1

Harris, R. F. (2015a). Effect of water potential on microbial growth and activity. In J. F. Parr, W. R. Gardner, & L. F. Elliott (Eds.), *SSSA Special Publications* (pp. 23–95). Soil Science Society of America. https://doi.org/10.2136/sssaspecpub9.c2

Hatfield, J. L., & Dold, C. (2019a). Water-use efficiency: Advances and challenges in a changing climate. *Frontiers in Plant Science*, *10*, 103. https://doi.org/10.3389/fpls.2019.00103

Havstad, K. M., Kustas, W. P., Rango, A., Ritchie, J. C., & Schmugge, T. J. (2000c). Jornada experimental range. *Remote Sensing of Environment*, *74*(1), 13–25. https://doi.org/10.1016/S0034-4257(00)00118-8

Herman, K. C., & Bleichrodt, R. (2022b). Go with the flow: Mechanisms driving water transport during vegetative growth and fruiting. *Fungal Biology Reviews*, *41*, 10–23. https://doi.org/10.1016/j.fbr.2021.10.002

Hillel, D. (2003). *Introduction to Environmental Soil Physics*. Elsevier.

Holden, P. A., & Fierer, N. (2005b). Vadose zone | microbial ecology. In *Encyclopedia of Soils in the Environment* (pp. 216–224). Elsevier. https://doi.org/10.1016/B0-12-348530-4/00172-7

Huang, Y., Wang, Y., Zhao, Y., Xu, X., Zhang, J., & Li, C. (2015b). Spatiotemporal distribution of soil moisture and salinity in the taklimakan desert highway shelterbelt. *Water*, *7*(12), 4343–4361. https://doi.org/10.3390/w7084343

Jabro, J., & Stevens, W. (2022). Soil-water characteristic curves and their estimated hydraulic parameters in no-tilled and conventionally tilled soils. Soil and Tillage Research, 219, 105342. https://doi.org/10.1016/j.still.2022.105342

Jia, Y.-H., & Shao, M.-A. (2014a). Dynamics of deep soil moisture in response to vegetational restoration on the Loess Plateau of China. *Journal of Hydrology*, *519*, 523–531. https://doi.org/10.1016/j.jhydrol.2014.07.043

Jiang, X., Wu, L., & Wei, Y. (2020b). Influence of fine content on the soil–water characteristic curve of unsaturated soils. *Geotechnical and Geological Engineering*, *38*(2), 1371–1378. https://doi.org/10.1007/s10706-019-01096-5

Jin, L., Quiroz, M., Garcia, A., Molina, V., Ramirez-Valle, O., Sosa, M., Orona, V., Kaip, G., Doser, D., Engle, M., Gutierrez, H., Darrouzet-Nardi, A., & Ma, L. (2022a). Tree size as a proxy of texture and soil salinity in a pecan orchard: Exploring the spatial variability and dominant controls on carbon fluxes in managed dryland critical zone. *Goldschmidt2022 Abstracts*. Goldschmidt2022, Honolulu, HI, USA. https://doi.org/10.46427/gold2022.11333

Jirků, V., Kodešová, R., Nikodem, A., Mühlhanselová, M., & Žigová, A. (2013a). Temporal variability of structure and hydraulic properties of topsoil of three soil types. *Geoderma*, *204–205*, 43–58. https://doi.org/10.1016/j.geoderma.2013.03.024

Kannenberg, S. A., Barnes, M. L., Bowling, D. R., Driscoll, A. W., Guo, J. S., & Anderegg, W. R. L. (2023b). Quantifying the drivers of ecosystem fluxes and water potential across the soil-plant-atmosphere continuum in an arid woodland. *Agricultural and Forest Meteorology*, *329*, 109269. https://doi.org/10.1016/j.agrformet.2022.109269

Katra, I., Blumberg, D. G., Lavee, H., & Sarah, P. (2007b). Spatial distribution dynamics of topsoil moisture in shrub microenvironment after rain events in arid and semi-arid areas by means of high-resolution maps. *Geomorphology*, *86*(3–4), 455–464. https://doi.org/10.1016/j.geomorph.2006.09.020

Kemp, P. R. (1983b). Phenological patterns of chihuahuan desert plants in relation to the timing of water availability. *The Journal of Ecology*, *71*(2), 427. https://doi.org/10.2307/2259725

Kemp, P. R., Reynolds, J. F., Pachepsky, Y., & Chen, J. (1997a). A comparative modeling study of soil water dynamics in a desert ecosystem. *Water Resources Research*, *33*(1), 73–90. https://doi.org/10.1029/96WR03015

Kirkham, M. (2023). Field capacity, wilting point, available water, and the nonlimiting water range. Principles of Soil and Plant Water Relations (Third Edition), 169-189. https://doi.org/10.1016/B978-0-323-95641-3.00013-1

Kirkham, M. B. (2005b). Field capacity, wilting point, available water, and the non-limiting water range. In *Principles of Soil and Plant Water Relations* (pp. 101–115). Elsevier. https://doi.org/10.1016/B978-012409751-3/50008-6

Knapp, A. K., Fahnestock, J. T., Hamburg, S. P., Statland, L. B., Seastedt, T. R., & Schimel, D. S. (1993b). Landscape patterns in soil-plant water relations and primary production in tallgrass prairie. *Ecology*, *74*(2), 549–560. https://doi.org/10.2307/1939315

Koley, S., & Jeganathan, C. (2020b). Estimation and evaluation of high spatial resolution surface soil moisture using multi-sensor multi-resolution approach. *Geoderma*, *378*, 114618. https://doi.org/10.1016/j.geoderma.2020.114618

Kool, D., Tong, B., Tian, Z., Heitman, J. L., Sauer, T. J., & Horton, R. (2019b). Soil water retention and hydraulic conductivity dynamics following tillage. *Soil and Tillage Research*, *193*, 95–100. https://doi.org/10.1016/j.still.2019.05.020

Kramer, P. J. (1974b). Fifty years of progress in water relations research. *Plant Physiology*, *54*(4), 463–471. https://doi.org/10.1104/pp.54.4.463

Kranner, I., Beckett, R., Hochman, A., & Nash, T. H. (2008). Desiccation-tolerance in lichens: A review. *The Bryologist*, *111*(4), 576–593. https://doi.org/10.1639/0007-2745-111.4.576

Lal, R., Kimble, J. M., Follett, R. F., & Stewart, B. A. (2018). *Soil Processes and the Carbon Cycle*. CRC Press.

Lee, E., Kumar, P., Knowles, J. F., Minor, R. L., Tran, N., Barron-Gafford, G. A., & Scott, R. L. (2021). Convergent hydraulic redistribution and groundwater access supported facilitative dependency between trees and grasses in a semi-arid environment. *Water Resources Research*, *57*(6), e2020WR028103. https://doi.org/10.1029/2020WR028103

Leib, B. G., Jabro, J. D., & Matthews, G. R. (2003b). Field evaluation and performance comparison of soil moisture sensors: *Soil Science*, *168*(6), 396–408. https://doi.org/10.1097/01.ss.0000075285.87447.86

Li, B., Wang, C., Gu, X., Zhou, X., Ma, M., Li, L., Feng, Z., Ding, T., Li, X., Jiang, T., Li, X., & Zheng, X. (2022b). Accuracy calibration and evaluation of capacitance-based

soil moisture sensors for a variety of soil properties. *Agricultural Water Management, 273*, 107913. https://doi.org/10.1016/j.agwat.2022.107913

Liang, H., Xue, Y., Shi, J., Li, Z., Liu, G., & Fu, B. (2018a). Soil moisture dynamics under *Caragana korshinskii* shrubs of different ages in Wuzhai County on the Loess Plateau, China. *Earth and Environmental Science Transactions of the Royal Society of Edinburgh*, *109*(3–4), 387–396. https://doi.org/10.1017/S1755691018000622

Liu, X., Liu, W., Tang, Q., Liu, B., Wada, Y., & Yang, H. (2022b). Global agricultural water scarcity assessment incorporating blue and green water availability under future climate change. *Earth's Future*, *10*(4), e2021EF002567. https://doi.org/10.1029/2021EF002567

Logsdon, S. D., & Cambardella, C. A. (2000b). Temporal changes in small depth-incremental soil bulk density. *Soil Science Society of America Journal*, *64*(2), 710–714. https://doi.org/10.2136/sssaj2000.642710x

Lopez, F. B., & Barclay, G. F. (2017b). Plant anatomy and physiology. In *Pharmacognosy* (pp. 45–60). Elsevier. https://doi.org/10.1016/B978-0-12-802104-0.00004-4

Lovett, G. M., Cole, J. J., & Pace, M. L. (2006b). Is net ecosystem production equal to ecosystem carbon accumulation? *Ecosystems*, *9*(1), 152–155. https://doi.org/10.1007/s10021-005-0036-3

Manzoni, S., Schimel, J. P., & Porporato, A. (2012b). Responses of soil microbial communities to water stress: Results from a meta-analysis. *Ecology*, *93*(4), 930–938. https://doi.org/10.1890/11-0026.1

McCluney, K. E., Belnap, J., Collins, S. L., González, A. L., Hagen, E. M., Nathaniel Holland, J., Kotler, B. P., Maestre, F. T., Smith, S. D., & Wolf, B. O. (2012b). Shifting species interactions in terrestrial dryland ecosystems under altered water availability and climate change. *Biological Reviews*, *87*(3), 563–582. https://doi.org/10.1111/j.1469-185X.2011.00209.x

McNamara, J. P., Chandler, D., Seyfried, M., & Achet, S. (2005b). Soil moisture states, lateral flow, and streamflow generation in a semi-arid, snowmelt-driven catchment. *Hydrological Processes*, *19*(20), 4023–4038. https://doi.org/10.1002/hyp.5869

METER Group AG (2016): KSAT Operation Manual. Available at: https://metergroup–83d0.kxcdn.com/app/uploads/2017/09/KSATManual-2017-10.pdf (last accessed: June 05, 2023). Olmstead, L. B., & Smith, W. O. (1970). *Water relations of Soils*, *water Relations of Soils*. https://naldc.nal.usda.gov/catalog/IND43893635 Retrieved May 5, 2023

Meter Group. (2016). PARIO automated soil particle size analyzer user manual. https://metergroup.com/enviro/pdfs/manuals/PARIO%20User%20Manual.pdf

Miller, D. E., & Bunger, Wm. C. (1963). Moisture retention by soil with coarse layers in the profile. *Soil Science Society of America Journal*, *27*(5), 586–589. https://doi.org/10.2136/sssaj1963.03615995002700050034x

Mueller, E. N., Wainwright, J., & Parsons, A. J. (2008b). Spatial variability of soil and nutrient characteristics of semi-arid grasslands and shrublands, Jornada Basin, New Mexico. *Ecohydrology*, *1*(1), 3–12. https://doi.org/10.1002/eco.1

Naylor, R. E. L. (2003b). *desiccation and survival in plants: Drying without dying* , eds m. B LACK & h. W. P RITCHARD . 416 pp. Wallingford, cabi (2002). £75. 00. Isbn 0 85199 534 9. *The Journal of Agricultural Science*, *140*(4), 489–489. https://doi.org/10.1017/S0021859603213393

Nemes, A., Schaap, M., Leij, F., & Wösten, J. (2001). Description of the unsaturated soil hydraulic database UNSODA version 2.0. Journal of Hydrology, 251(3-4), 151-162. https://doi.org/10.1016/S0022-1694(01)00465-6

Nimmo, J. R. (2005a). Porosity and pore-size distribution. In *Encyclopedia of Soils in the Environment* (pp. 295–303). Elsevier. https://doi.org/10.1016/B0-12-348530-4/00404-5

Niu, G., Kong, L., Miao, Y., Li, X., & Chen, F. (2024). A Modified Method for the Fredlund and Xing (FX) Model of Soil-Water Retention Curves. Processes, 12(1), 50. https://doi.org/10.3390/pr12010050

Novick, K. A., Ficklin, D. L., Baldocchi, D., Davis, K. J., Ghezzehei, T. A., Konings, A. G., MacBean, N., Raoult, N., Scott, R. L., Shi, Y., Sulman, B. N., & Wood, J. D. (2022b). Confronting the water potential information gap. *Nature Geoscience*, *15*(3), 158–164. https://doi.org/10.1038/s41561-022-00909-2

Noy-Meir, I. (1973b). Desert ecosystems: Environment and producers. *Annual Review of Ecology and Systematics*, *4*(1), 25–51. https://doi.org/10.1146/annurev.es.04.110173.000325

Onyelowe, K. C., Mojtahedi, F. F., Azizi, S., Mahdi, H. A., Sujatha, E. R., Ebid, A. M., Darzi, A. G., & Aneke, F. I. (2022b). Innovative overview of swrc application in modeling geotechnical engineering problems. *Designs*, *6*(5), 69. https://doi.org/10.3390/designs6050069

Ortiz, A. C., Jin, L., Ogrinc, N., Kaye, J., Krajnc, B., & Ma, L. (2022b). Dryland irrigation increases accumulation rates of pedogenic carbonate and releases soil abiotic CO_2. *Scientific Reports*, *12*(1), 464. https://doi.org/10.1038/s41598-021-04226-3

Osman, K. T. (2013b). Physical properties of soil. In K. T. Osman, *Soils* (pp. 49–65). Springer Netherlands. https://doi.org/10.1007/978-94-007-5663-2_5

Othman, Y., VanLeeuwen, D., Heerema, R., & St. Hilaire, R. (2014b). Midday stem water potential values needed to maintain photosynthesis and leaf gas exchange established

for pecan. *Journal of the American Society for Horticultural Science*, *139*(5), 537–546. https://doi.org/10.21273/JASHS.139.5.537

Pan, W., Boyles, R. P., White, J. G., & Heitman, J. L. (2012b). Characterizing soil physical properties for soil moisture monitoring with the north carolina environment and climate observing network. *Journal of Atmospheric and Oceanic Technology*, *29*(7), 933–943. https://doi.org/10.1175/JTECH-D-11-00104.1

Pérez-de-los-Reyes, C., Sánchez-Ormeño, M., Bravo Martín-Consuegra, S., García-Pradas, J., Pérez-de-los-Reyes, M. L., Ramírez, A., Ortíz-Villajos, J. Á. A., García Navarro, F. J., & Jiménez-Ballesta, R. (2022b). The influence of depth on the water retention properties of vineyard soils. *Agricultural Water Management*, *261*, 107384. https://doi.org/10.1016/j.agwat.2021.107384

Pérez-Ruiz, E. R., Vivoni, E. R., & Sala, O. E. (2022b). Seasonal carryover of water and effects on carbon dynamics in a dryland ecosystem. *Ecosphere*, *13*(7), e4189. https://doi.org/10.1002/ecs2.4189

Peters, A., & Durner, W. (2008b). Simplified evaporation method for determining soil hydraulic properties. *Journal of Hydrology*, *356*(1–2), 147–162. https://doi.org/10.1016/j.jhydrol.2008.04.016

Phillips, F. M., & Castro, M. C. (2003a). Groundwater dating and residence-time measurements. In *Treatise on Geochemistry* (pp. 451–497). Elsevier. https://doi.org/10.1016/B0-08-043751-6/05136-7

Pockman, W. T., & Small, E. E. (2010a). The influence of spatial patterns of soil moisture on the grass and shrub responses to a summer rainstorm in a chihuahuan desert ecotone. *Ecosystems*, *13*(4), 511–525. https://doi.org/10.1007/s10021-010-9337-2

Potts, M., & Friedmann, E. I. (1981). Effects of water stress on cryptoendolithic cyanobacteria from hot desert rocks. *Archives of Microbiology*, *130*(4), 267–271. https://doi.org/10.1007/BF00425938

Qi, M. Q., & Redmann, R. E. (1993b). Seed germination and seedling survival of C3 and C4 grasses under water stress. *Journal of Arid Environments*, *24*(3), 277–285. https://doi.org/10.1006/jare.1993.1024

Randerson, J. T., Chapin, F. S., Harden, J. W., Neff, J. C., & Harmon, M. E. (2002b). Net ecosystem production: A comprehensive measure of net carbon accumulation by ecosystems. *Ecological Applications*, *12*(4), 937–947. https://doi.org/10.1890/1051-0761(2002)012[0937:NEPACM]2.0.CO;2

Rasheed, M. W., Tang, J., Sarwar, A., Shah, S., Saddique, N., Khan, M. U., Imran Khan, M., Nawaz, S., Shamshiri, R. R., Aziz, M., & Sultan, M. (2022b). Soil moisture measuring techniques and factors affecting the moisture dynamics: A comprehensive review. *Sustainability*, *14*(18), 11538. https://doi.org/10.3390/su141811538

Reed, S., Ferrenberg, S., Collins, S. L., & Sala, O. (2018b). *The pulse-reserve paradigm and explaining dryland function: Past, present, and future*. *2018*, B31D-04. https://ui.adsabs.harvard.edu/abs/2018AGUFM.B31D..04R

Reynolds, J. F., Kemp, P. R., Ogle, K., & Fernández, R. J. (2004b). Modifying the 'pulse–reserve' paradigm for deserts of North America: Precipitation pulses, soil water, and plant responses. *Oecologia*, *141*(2), 194–210. https://doi.org/10.1007/s00442-004-1524-4

Rezaur, R. B., Rahardjo, H., & Leong, E. C. (2002b). Spatial and temporal variability of pore-water pressures in residual soil slopes in a tropical climate. *Earth Surface Processes and Landforms*, *27*(3), 317–338. https://doi.org/10.1002/esp.322

Robinson, D. A., Campbell, C. S., Hopmans, J. W., Hornbuckle, B. K., Jones, S. B., Knight, R., Ogden, F., Selker, J., & Wendroth, O. (2008b). Soil moisture measurement for ecological and hydrological watershed-scale observatories: A review. *Vadose Zone Journal*, *7*(1), 358–389. https://doi.org/10.2136/vzj2007.0143

Robinson, D. A., Cooper, J. D., & Gardner, C. M. K. (2002b). Modelling the relative permittivity of soils using soil hygroscopic water content. *Journal of Hydrology*, *255*(1–4), 39–49. https://doi.org/10.1016/S0022-1694(01)00508-X

Roth, C. H. (1997b). Bulk density of surface crusts: Depth functions and relationships to texture. *CATENA*, *29*(3–4), 223–237. https://doi.org/10.1016/S0341-8162(96)00071-9

Rowlandson, T. L., Berg, A. A., Bullock, P. R., Ojo, E. R., McNairn, H., Wiseman, G., & Cosh, M. H. (2013b). Evaluation of several calibration procedures for a portable soil moisture sensor. *Journal of Hydrology*, *498*, 335–344. https://doi.org/10.1016/j.jhydrol.2013.05.021

Rudiyanto, Minasny, B., Chaney, N. W., Maggi, F., Goh Eng Giap, S., Shah, R. M., Fiantis, D., & Setiawan, B. I. (2021). Pedotransfer functions for estimating soil hydraulic properties from saturation to dryness. *Geoderma*, *403*, 115194. https://doi.org/10.1016/j.geoderma.2021.115194

S.U., S. L., Singh, D. N., & Shojaei Baghini, M. (2014a). A critical review of soil moisture measurement. *Measurement*, *54*, 92–105. https://doi.org/10.1016/j.measurement.2014.04.007

Saffari, R., Nikooee, E., Habibagahi, G., & Van Genuchten, M. Th. (2019b). Effects of biological stabilization on the water retention properties of unsaturated soils. *Journal of Geotechnical and Geoenvironmental Engineering*, *145*(7), 04019028. https://doi.org/10.1061/(ASCE)GT.1943-5606.0002053

Sala, O. E., Lauenroth, W. K., Parton, W. J., & Trlica, M. J. (1981b). Water status of soil and vegetation in a shortgrass steppe. *Oecologia*, *48*(3), 327–331. https://www.jstor.org/stable/4216318

Sanchez, P. A. (2019). *Properties and management of soils in the tropics* (2nd ed.). Cambridge University Press. https://doi.org/10.1017/9781316809785

Sauer, R. H., Warner, M. L., & Hinds, W. T. (1984a). Indirect determination of rooting depth and permanent wilting point. *Ecological Modelling*, *21*(1–2), 109–124. https://doi.org/10.1016/0304-3800(84)90027-9

Schindler, U., & Müller, L. (2006). Simplifying the evaporation method for quantifying soil hydraulic properties. Journal of Plant Nutrition and Soil Science, 169(5), 623-629. https://doi.org/10.1002/jpln.200521895

Schlaepfer, D. R., Lauenroth, W. K., & Bradford, J. B. (2012b). Ecohydrological niche of sagebrush ecosystems. *Ecohydrology*, *5*(4), 453–466. https://doi.org/10.1002/eco.238

Setia, R., & Marschner, P. (2013b). Impact of total water potential and varying contribution of matric and osmotic potential on carbon mineralization in saline soils. *European Journal of Soil Biology*, *56*, 95–100. https://doi.org/10.1016/j.ejsobi.2013.02.003

Shah, P., & Singh, D. (2006b). Methodology for determination of hygroscopic moisture content of soils. *Journal of ASTM International*, *3*(2), 1–14. https://doi.org/10.1520/JAI13376

Sharma, K., Irmak, S., & Kukal, M. S. (2021b). Propagation of soil moisture sensing uncertainty into estimation of total soil water, evapotranspiration and irrigation decision-making. *Agricultural Water Management*, *243*, 106454. https://doi.org/10.1016/j.agwat.2020.106454

Silva, L. C. R., & Lambers, H. (2021b). Soil-plant-atmosphere interactions: Structure, function, and predictive scaling for climate change mitigation. *Plant and Soil*, *461*(1–2), 5–27. https://doi.org/10.1007/s11104-020-04427-1

SoilView analysis (version 2.0.1) [Computer software]. (2022). Developed by SoilView LLC. https://www.soilview.com/analysis

SOP. (2021). Gravimetric θ calculations. https://margenot.cropsciences.illinois.edu/methods-sops/. Soils Laboratory, University of Illinois.

Sosa, E., Ma, L., Engle, M., & Jin, L. (2023a). *Mobility of trace elements underneath irrigated agricultural fields: Implication of dryland soil and water quality along the Rio Grande Valley*. https://doi.org/10.21203/rs.3.rs-2556954/v1

Sparks, D. L. (2018). *Advances in agronomy* (1st ed), *148*. Academic Press.

Stark, J. M., & Firestone, M. K. (1995a). Mechanisms for soil moisture effects on activity of nitrifying bacteria. *Applied and Environmental Microbiology*, *61*(1), 218–221. https://doi.org/10.1128/aem.61.1.218-221.1995

Stefan, G., Cornelia, B., Jörg, R., & Michael, B. (2014b). Soil water availability strongly alters the community composition of soil protists. *Pedobiologia*, *57*(4–6), 205–213. https://doi.org/10.1016/j.pedobi.2014.10.001

Studio Team. (2021). *RStudio: Integrated development for R. RStudio*. PBC version 1.4.1106.

Sun, F., Xiao, B., Li, S., & Kidron, G. J. (2021a). Towards moss biocrust effects on surface soil water holding capacity: Soil water retention curve analysis and modeling. *Geoderma*, *399*, 115120. https://doi.org/10.1016/j.geoderma.2021.115120

Too, V. K., Omuto, C. T., Biamah, E. K., & Obiero, J. P. (2014b). Review of soil water retention characteristic (Swrc) models between saturation and oven dryness. *Open Journal of Modern Hydrology*, *04*(04), 173–182. https://doi.org/10.4236/ojmh.2014.44017

University of Zagreb, Faculty of Agriculture, Svetošimunska cesta 25, HR-10000 Zagreb, Croatia, Bogunović, I., Đekmeti, I., Magdić, I., Vrbanić, M., Matošić, S., & Mesić, M. (2016). Spatial modelling for describing spatial variability of soil physical properties in eastern Croatia. *Poljoprivreda*, *22*(1), 46–52. https://doi.org/10.18047/poljo.22.1.7

Van Genuchten, M. T. (1980). A Closed-form Equation for Predicting the Hydraulic Conductivity of Unsaturated Soils. Soil Science Society of America Journal, 44(5), 892-898. https://doi.org/10.2136/sssaj1980.03615995004400050002x

Varble, J. L., & Chávez, J. L. (2011a). Performance evaluation and calibration of soil water content and potential sensors for agricultural soils in eastern Colorado. *Agricultural Water Management*, *101*(1), 93–106. https://doi.org/10.1016/j.agwat.2011.09.007

Vegetation models for climate change impacts | Climate change resource center. (2023). Retrieved February 10, 2023. https://www.fs.usda.gov/ccrc/topics/overview-vegetation-models

Verstraeten, W., Veroustraete, F., & Feyen, J. (2008b). Assessment of evapotranspiration and soil moisture content across different scales of observation. *Sensors*, *8*(1), 70–117. https://doi.org/10.3390/s8010070

Veste, M., Staudinger, M., & Küppers, M. (2008c). Spatial and temporal variability of soil water in drylands: Plant water potential as a diagnostic tool. *Forestry Studies in China*, *10*(2), 74–80. https://doi.org/10.1007/s11632-008-0022-x

Volume information. (1943b). *The American Midland Naturalist*, *30*(3). https://www.jstor.org/stable/2421202

Wan, C., & Sosebee, R. E. (1991a). Water relations and transpiration of honey mesquite on 2 sites in west texas. *Journal of Range Management*, *44*(2), 156. https://doi.org/10.2307/4002315

Wang, C., Wang, S., Fu, B., Yang, L., & Li, Z. (2017b). Soil moisture variations with land use along the precipitation gradient in the north–south transect of the loess plateau. *Land Degradation & Development*, *28*(3), 926–935. https://doi.org/10.1002/ldr.2604

Wang, C., Zhao, C., Xu, Z., Wang, Y., & Peng, H. (2013b). Effect of vegetation on soil water retention and storage in a semi-arid alpine forest catchment. *Journal of Arid Land*, *5*(2), 207–219. https://doi.org/10.1007/s40333-013-0151-5

Wang, S., Fu, B. J., Gao, G. Y., Yao, X. L., & Zhou, J. (2012b). Soil moisture and evapotranspiration of different land cover types in the Loess Plateau, China. *Hydrology and Earth System Sciences*, *16*(8), 2883–2892. https://doi.org/10.5194/hess-16-2883-2012

Wang, Y., Ma, J., & Guan, H. (2016a). A mathematically continuous model for describing the hydraulic properties of unsaturated porous media over the entire range of matric suctions. *Journal of Hydrology*, *541*, 873–888. https://doi.org/10.1016/j.jhydrol.2016.07.046

Weather averages for El Paso, Texas. (2023). Retrieved 26 May 2023, from https://www.usclimatedata.com/climate/el-paso/texas/united-states/ustx0413

Wei, F., Wang, S., Fu, B., Wang, L., Liu, Y. Y., & Li, Y. (2019a). African dryland ecosystem changes controlled by soil water. *Land Degradation & Development*, *30*(13), 1564–1573. https://doi.org/10.1002/ldr.3342

Wendroth, O., Pohl, W., Koszinski, S., Rogasik, H., Ritsema, C. J., & Nielsen, D. R. (1999b). Spatio-temporal patterns and covariance structures of soil water status in two Northeast-German field sites. *Journal of Hydrology*, *215*(1–4), 38–58. https://doi.org/10.1016/S0022-1694(98)00260-1

Weverka, J., Runte, G. C., Porzig, E. L., & Carey, C. J. (2023a). Exploring plant and soil microbial communities as indicators of soil organic carbon in a California rangeland. *Soil Biology and Biochemistry*, *178*, 108952. https://doi.org/10.1016/j.soilbio.2023.108952

Whalley, W. R., Ober, E. S., & Jenkins, M. (2013a). Measurement of the matric potential of soil water in the rhizosphere. *Journal of Experimental Botany*, *64*(13), 3951–3963. https://doi.org/10.1093/jxb/ert044

Wiecheteck, L. H., Giarola, N. F. B., De Lima, R. P., Tormena, C. A., Torres, L. C., & De Paula, A. L. (2020b). Comparing the classical permanent wilting point concept of soil (−15,000 hPa) to biological wilting of wheat and barley plants under contrasting soil textures. *Agricultural Water Management*, *230*, 105965. https://doi.org/10.1016/j.agwat.2019.105965

Williams, M. A., & Rice, C. W. (2007b). Seven years of enhanced water availability influences the physiological, structural, and functional attributes of a soil microbial

community. *Applied Soil Ecology*, *35*(3), 535–545. https://doi.org/10.1016/j.apsoil.2006.09.014

Wilson, J. M., & Griffin, D. M. (1975a). Water potential and the respiration of microorganisms in the soil. *Soil Biology and Biochemistry*, *7*(3), 199–204. https://doi.org/10.1016/0038-0717(75)90038-3

Wösten, J., Pachepsky, Y., & Rawls, W. (2001). Pedotransfer functions: Bridging the gap between available basic soil data and missing soil hydraulic characteristics. Journal of Hydrology, 251(3-4), 123-150. https://doi.org/10.1016/S0022-1694(01)00464-4

Wuddivira, M. N., Robinson, D. A., Lebron, I., Bréchet, L., Atwell, M., De Caires, S., Oatham, M., Jones, S. B., Abdu, H., Verma, A. K., & Tuller, M. (2012b). Estimation of soil clay content from hygroscopic water content measurements. *Soil Science Society of America Journal*, *76*(5), 1529–1535. https://doi.org/10.2136/sssaj2012.0034

Xiao, J., Chen, J., Davis, K. J., & Reichstein, M. (2012b). Advances in upscaling of eddy covariance measurements of carbon and water fluxes. *Journal of Geophysical Research: Biogeosciences*, *117*(G1), 2011JG001889. https://doi.org/10.1029/2011JG001889

Zeitoun, R., Vandergeest, M., Vasava, H. B., Machado, P. V. F., Jordan, S., Parkin, G., Wagner-Riddle, C., & Biswas, A. (2021c). In-situ estimation of soil water retention curve in silt loam and loamy sand soils at different soil depths. *Sensors*, *21*(2), 447. https://doi.org/10.3390/s21020447

Zhang, X., Zhang, X., & Li, G. (2015a). The effect of texture and irrigation on the soil moisture vertical-temporal variability in an urban artificial landscape: A case study of Olympic Forest Park in Beijing. *Frontiers of Environmental Science & Engineering*, *9*(2), 269–278. https://doi.org/10.1007/s11783-014-0672-y

Zhao, Y., Peth, S., Wang, X. Y., Lin, H., & Horn, R. (2010a). Controls of surface soil moisture spatial patterns and their temporal stability in a semi-arid steppe. *Hydrological Processes*, *24*(18), 2507–2519. https://doi.org/10.1002/hyp.7665

Zheng, C., Jia, L., & Zhao, T. (2023a). A 21-year dataset (2000–2020) of gap-free global daily surface soil moisture at 1-km grid resolution. *Scientific Data*, *10*(1), 139. https://doi.org/10.1038/s41597-023-01991-w

VITA

Lindsey R. Dacey was awarded her Bachelor of Science in biological sciences with a concentration in ecology and evolution from the University of Texas at El Paso in 2019. As an undergraduate, she conducted research on soil respiration with a primary focus on Nitrogen under the mentorship of Dr. Anthony Darrouzet-Nardi. Post-graduation, Lindsey worked for the El Paso Fire Department as a contact tracer for two years. Following this, she was admitted into the master's Program in Environmental Science at the University of Texas at El Paso under the Department of Earth, Environmental, and Resource Sciences in 2021. Through her graduate program, she worked as a master's teaching assistant for courses in hydrology, physical geology labs, and environmental science. Her research focused on water sufficiency for organismal function in dryland critical zones, as this has served as a basis of her thesis it has also inspired her to further her career in related studies.

Contact Information : lrdacey@miners.utep.edu